IJARCCE ISSN (O) 2278-1021, ISSN (P) 2319-5940

International Journal of Advanced Research in Computer and Communication Engineering

Impact Factor 8.102 ⁜ Peer-reviewed & Refereed journal ⁜ Vol. 13, Issue 11, November 2024

DOI: 10.17148/IJARCCE.2024.131101

Research on Indoor Wireless Localization Algorithm in FTTR WLAN Scenerio

Binga Kanvalga Ishaku[1], Mayamba Wakaye Maxwell[2], Wakaye Abba Maxwell[3], Jahleel Alhamdu Durami [4], Yakubu Ernest Nwuku [5]

Department of Information and Communication Engineering, Huazhong University of Science and Technology, Wuhan, China[1]

Department of Computer Science, Bingham University,Nasarawa,Nigeria[2]

Department of Computer Science,Chongqing University of Posts and Telecommunications,Chongqing,China[3]

Department of Digital Design and Manufacturing, Metropolitan University, Manchester, United Kingdom[4]

Department of Computer Science,Federal University Wukari,Taraba, Nigeria[5]

Abstract: Wireless indoor positioning has been widely adopted in extensive practice for its highly accurate and reliable characteristics. However, in order to achieve good positioning accuracy, positioning algorithms must be designed to be compatible with wireless positioning facilities. With the application of 802.11 ax protocol, the available bandwidth of wireless network transmission system will increase from 80 MHz to 160 MHz compared to the previous system. in addition, more access points are deployed within the indoor area, resulting in serious impact on high-frequency signal attenuation caused by interference and wall penetration for high-precision indoor positioning. In addition, the added 5.8GHz transmission signal lacks a common effective data set to support positioning functions, posing a great challenge for researchers of FTTR-based scenarios for positioning.

For indoor wireless communication network systems, this study proposes a ray-tracing model-based 5.8 GHz data set assembly method. The method includes simulating access points to generate reference signals, performing endpoint channel estimation, and generating frequency response images. The frequency response matrix is generated within the available bandwidth of FTTR with the help of existing WiFi positioning datasets. To achieve high-precision indoor localization, this study further proposes a deep neural network (DNN) computation method based on parallel path principal component analysis (PCA) preprocessing. The method includes the preprocessing step of parallel path PCA, the training process of the DNN network, and the user location calculation. The classification matrix is generated using principal component analysis (PCA) of parallel paths by using a fully connected neural network for training to improve the localization accuracy. Experimental results show that the proposed localization algorithm achieves a localization accuracy of less than 1 meter, which is not only more accurate than the traditional location estimation algorithm, but also meets the demand for fine-grained localization in practical applications.

Keywords: Indoor positioning, Wi-Fi, FTTR, PCA, DNN networks.

I. INTRODUCTION

A. *BACKGROUND*

The emergence of indoor applications such as online education, interactive online gaming, and augmented/virtual reality (AR/VR) have created a significant challenge for designing the sixth-generation (6G) indoor wireless networks. These applications have stringent requirements for not only extremely high data rate but also ultra-low end-to-end network latency, which means that the wireless networks must be able to transmit large amounts of data quickly while also minimizing the time it takes for data to travel from the sender to the receiver.

Fiber-to-The-Room (FTTR) wireless local area networks (WLANs) have been identified by the International Telecommunication Union (ITU) as a promising solution for meeting these requirements**Error! Reference source not found.**. The FTTR WLAN enables dense deployment of access points (APs), referred to as optical network units (ONUs), which are interconnected using a high-capacity passive optical network (PON). This allows for high-speed data transmission with minimal latency, which is critical for applications such as online gaming and AR/VR.

DOI: 10.17148/IJARCCE.2024.131101

FTTR WLAN is a novel indoor wireless network technology that offers high-speed, low-latency connectivity by utilizing a unique architecture that allows for dense deployment of optical network units (ONUs). Unlike traditional WLANs, where mobile devices can only access the nearest AP or the AP with the highest signal strength, FTTR WLANs enable mobile devices to connect to any ONU within its communication range in a flexible and probabilistic manner, thanks to the use of basic service set (BSS) coloring technique introduced in IEEE 802.11ax WLAN.

This flexibility in accessing multiple ONUs reduces the probability of collisions during data packet transmissions, which is especially crucial for emerging indoor applications such as online education, interactive online gaming, and augmented/virtual reality (AR/VR) that have stringent requirements for ultra-low end-to-end network latency. Furthermore, FTTR WLANs employ efficient spatial frequency reuse across the ONUs, enabling full reuse of the same frequency band across all ONUs for wireless channel access and communication. This significantly improves the data rate, spectral efficiency, and energy efficiency of indoor wireless networks.

One key advantage of FTTR WLAN is the use of the basic service set (BSS) coloring technique, which was introduced in the IEEE 802.11ax WLAN. This technique allows for full reuse of the same frequency band across all ONUs for wireless channel access and communication, enabling mobile devices to flexibly access multiple ONUs in a probabilistic manner to mitigate collisions during carrier sense multiple access with collision avoidance (CSMA/CA) based data transmission. This means that mobile devices can connect to the ONUs with the strongest signals and can quickly switch to other ONUs if the signal strength decreases, ensuring a reliable and consistent wireless connection.

Moreover, FTTR WLAN significantly improves the data rate, spectral, and energy efficiency of indoor wireless networks by reducing communication distances between mobile devices and the ONUs, as well as efficient spatial frequency reuse. The dense deployment of ONUs allows for more efficient use of the available frequency spectrum, resulting in increased data rates and reduced energy consumption.a

In addition, in the FTTR WLAN scenario, the frequency band for data transmission between the ONU and the user is increased from the original 80MHz to 160MHz, and the existing positioning algorithm using the RSSI fingerprint data set based on the 80MHz bandwidth will bring a large one error in the 160MHz bandwidth. For example, in the 5.8GHz band, the data transmission is easily affected by walls and occlusions, resulting in less accurate RSSI fingerprint data received by users. Moreover, at present, most of the 5.8GHz spectrum is used in industrial IoT, and the popularity of indoor 5.8GHz band is not high enough. Therefore, there is a lack of corresponding RSSI fingerprint data set for research and positioning. How to accurately locate the user position indoors in 160MHz bandwidth has also become a key research problem in FTTR WLAN scenario.

In summary, the FTTR WLAN is a promising solution for meeting the stringent requirements of emerging indoor applications, such as online education, interactive online gaming, and AR/VR. With its high-speed data transmission, minimal latency, and efficient use of frequency spectrum, it has the potential to significantly improve the user experience for indoor communications.

B. INTRODUCTION for FTTR WLAN

FTTR WLAN contains two parts, one is the PON optical network, and the other is the wireless network part. The next part will be introduced and stated according to the above two parts.

IJARCCE ISSN (O) 2278-1021, ISSN (P) 2319-5940

International Journal of Advanced Research in Computer and Communication Engineering

Impact Factor 8.102 ⁜ Peer-reviewed & Refereed journal ⁜ Vol. 13, Issue 11, November 2024

DOI: 10.17148/IJARCCE.2024.131101

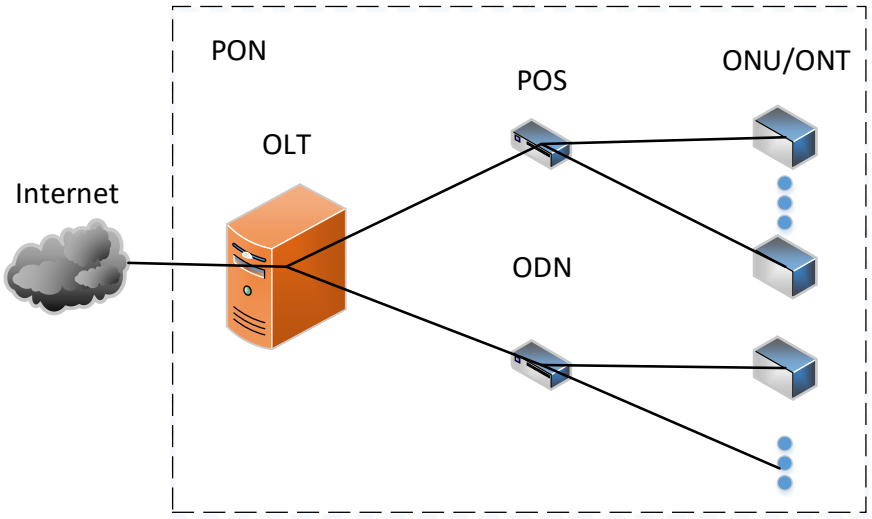

Figure 1.1 GPON system reference configuration diagram

1. *PON OPTICAL NETWORK:*

PON**Error! Reference source not found.-Error! Reference source not found.** (Passive Optical Network) is an optical fiber transmission technology, which transmits data to end-user's home or office through fiber optic network.PON technology mainly consists of optical transmission unit (OLT), optical network unit (ONU) and optical fiber. Compared with the traditional copper network, PON technology has higher bandwidth, lower transmission latency and greater stability, as show in Figure 1.1.

Passive optical network (PON) is a high-speed, cost-effective, and energy-efficient network architecture widely deployed in telecommunication networks. The PON network comprises several essential components that work in tandem to provide high-quality network services to users**Error! Reference source not found.**.

1) The Optical Line Terminal (OLT) is a vital component of the PON network that serves as the gateway between the PON and external networks. It is responsible for managing and controlling the network, providing users with efficient and centralized network services. The OLT connects to the Optical Network Units (ONUs)/Optical Network Terminals (ONTs) via the Optical Distribution Network (ODN).

2) The ONU/ONT is a component located at the user's end, which provides network access services to users. It enables users to access high-speed internet services by connecting their devices to the PON network. The ONU/ONT converts optical signals transmitted through the ODN into electrical signals and sends them to the user's device.

3) The Optical Distribution Network (ODN) is a passive network composed of optical fibers, splitters, and connectors that connect the OLT to the ONUs/ONTs. The ODN plays a crucial role in propagating the optical signals between the OLT and ONUs/ONTs. It ensures that the data transmission is stable, reliable, and secure.

There are several different types of PON technology, including EPON**Error! Reference source not found.Error! Reference source not found.** (Ethernet PON), GPON **Error! Reference source not found.**(Gigabit PON) and 10G PON, etc. EPON technology is an Ethernet protocol-based PON technology that can provide bandwidth speeds of up to 1 Gbps. GPON technology is a PON technology that uses the ITU-T G.984 standard and 10G PON technology is a PON technology that can provide 10 Gbps bandwidth speed, which can meet the needs of high bandwidth applications.

Time division multiplexed passive optical network (TDM-PON)**Error! Reference source not found.-Error! Reference source not found.** is a popular technology that enables the provision of broadband access services to end devices/users and has been widely deployed globally. TDM-PON consists of an optical line terminal (OLT) located in the central office (CO) of the network operator, which connects customer-side multiple optical network units (ONUs) through tree-topology fiber links.

In the upstream (US) direction from ONUs to OLT, the bandwidth of the fiber link is shared among all connected ONUs

DOI: 10.17148/IJARCCE.2024.131101

in a TDM manner. Each ONU sends its US frame during a dedicated time slot assigned by the OLT, which uses dynamic bandwidth allocation (DBA) scheme to decide each ONU's dedicated US transmission slot. This allows for efficient use of the available bandwidth and ensures that each ONU receives fair access to the available resources.

In the downstream (DS) direction, the OLT broadcasts DS frames to all ONUs, and each ONU filters out its belonging DS frames using a logical link identifier in EPON. This broadcast nature of the DS transmission allows for efficient use of the available bandwidth and simplifies the network design.

Ethernet PON (EPON) and Gigabit PON (GPON) are two popular types of TDM-PONs. EPON is a cost-effective solution that uses Ethernet frames for both US and DS transmission, while GPON is a high-speed solution that uses Asynchronous Transfer Mode (ATM) cells for DS transmission and GEM frames for US transmission.

TDM-PON has several advantages over other access network technologies, including high bandwidth, low latency, and high reliability. It is also a scalable solution that can accommodate a large number of ONUs, making it suitable for use in densely populated areas.

In EPON-based access networks, the tree-and-branch topology is the most common and typically consists of one OLT and several ONUs. The fiber length between the OLT and the ONUs usually ranges from 10 km to 100 km, depending on the specific deployment scenario. As the central node in the network, the OLT is responsible for managing both downstream (DS) and upstream (US) transmissions of all ONUs and scheduling network resources. In traditional PONs with a fixed polling sequence, the OLT broadcasts GATE messages and DS data to all ONUs, and allocates their US bandwidth based on the time window (TW) specified in the ONUs' REPORT messages. In EPONs, each ONU uses a unique logical link identifier (LLID) to receive its DS data. In the US direction, ONUs transmit their US data to the OLT in a TDM way, one by one. The OLT assigns each ONU a specific US time slot based on its REPORT message and adjusts the bandwidth allocation dynamically using the dynamic bandwidth allocation (DBA) scheme. The OLT also performs the function of detecting collisions and allocating resources to mitigate collisions in the network. Overall, the EPON-based access network with TDM-PON architecture provides a high-capacity and reliable broadband access solution for end-users, and has been widely adopted in various applications such as Internet access, video streaming, and cloud computing.

2. WIRELESS NETWORK:

Throughout the FTTR WLAN, data transmission from the ONU to the user is performed using wireless network transmission.

Wi-Fi**Error! Reference source not found.-Error! Reference source not found.**, also known as Wireless Fidelity, is a popular wireless networking technology that enables devices to communicate with each other without the need for physical cables. It operates on the IEEE 802.11 standard and uses radio waves to transmit data between devices over a wireless network.

Wi-Fi networks can be set up in a variety of environments, such as homes, offices, and public spaces like cafes, airports, and hotels. These networks enable devices such as smartphones, laptops, tablets, and smart home devices to connect to the internet and communicate with each other.

The Wi-Fi standard specifies various specifications for wireless network transmission, such as the frequency band, data transfer rates, and security protocols. The most commonly used frequency bands for Wi-Fi networks are 2.4 GHz and 5 GHz, which offer different advantages and disadvantages. The 2.4 GHz band offers better coverage but lower data transfer rates, while the 5 GHz band offers higher data transfer rates but less coverage.

The latest Wi-Fi standards have not only improved speed, range, and security, but they have also introduced new technologies such as Multiple Input Multiple Output (MIMO)**Error! Reference source not found.Error! Reference source not found.** and Orthogonal Frequency Division Multiple Access (OFDMA)**Error! Reference source not found.Error! Reference source not found.**. MIMO uses multiple antennas to transmit and receive data, while OFDMA allows multiple devices to share the same frequency at the same time, improving network efficiency and reducing latency.

Furthermore, the latest Wi-Fi standards also support beamforming, which is a technology that allows the Wi-Fi access point to direct the wireless signal towards the device, rather than broadcasting the signal in all directions. This results in

DOI: 10.17148/IJARCCE.2024.131101

a stronger and more stable signal, particularly at longer ranges.

Wi-Fi networks can also use various security protocols such as WEP, WPA, and WPA2 to protect against unauthorized access, eavesdropping, and other security threats. These protocols use encryption and authentication methods to secure data transfer and prevent unauthorized access to the network.

One of the primary advantages of Wi-Fi networks is their convenience and flexibility. They allow for wireless communication between devices, which enables mobility and reduces the clutter of cables. This is particularly useful in environments such as homes and offices where devices need to be moved around frequently.

Another advantage of Wi-Fi networks is their scalability. They can be easily expanded by adding more access points or routers to the network, making it possible to cover larger areas or accommodate more devices.

C. MOTIVATION

Improvement is needed in terms of accuracy for WiFi fingerprint high precision indoor scheme for FTTR scenarios. Location-based Services (LBS) have grown in popularity as a result of the widespread usage of smart devices in our daily lives, including laptops, iPads, and PDAs. The need for indoor LBSs is currently significant, which propels the development of location computing technologies. Due to the growing popularity of smart structures and gadgets, the navigation systems and indoor positioning sectors have experienced fast growth in recent years. As is presented in this work, there are many indoor positioning systems that exist using a wide variety of technologies and there are advantages and disadvantages for each of those systems. The aim of this research is to show that WiFi fingerprint presented in this work provides better accuracy compared to existing systems. The relevance to the society in general lies in that there are several market segments and emerging technologies that can take full advantage of WiFi fingerprint technologies. Indoor positioning systems can be used for applications such as location-based shopping and advertising, and even for emergency response applications.

Practically speaking, indoor localization will considerably enhance network administration, healthcare monitoring, emergency personnel navigation, and security. Numerous indoor locating technologies, including WLAN, Ultrasound, Lighting, RFID, and Bluetooth, have been marketed. The majority of the above-mentioned techniques demand significant infrastructure and transceiver deployments, which raises maintenance expenses. However, WLAN fingerprinting-based techniques have been embraced by many academics for three reasons. First off, most large buildings already have WLAN services available as a foundation for wireless network coverage, so additional hardware and expenses are not necessary when it is used for an Indoor Positioning System (IPS). WLAN services operate at a 2.4GHz Industrial, Scientific, and Medical (ISM) band within a range of 50-100 m. Second, most wireless receivers and mobile devices have Networking Interface Cards (NIC) that can measure RSS values. Third, due of a multi-path fading problem, the path loss model-based solution does not function correctly inside buildings. This issue arises from the exceedingly complicated nature of signal propagation in indoor situations and the fact that RSS signal intensity at any one site typically varies with the surrounding circumstances.

Furthermore, in the FTTR WLAN scenario, the frequency range for transmitting data between the Optical Network Unit (ONU) and the user has been expanded from the original 80MHz to 160MHz. However, the existing positioning algorithm that relies on the RSSI fingerprint dataset, which was developed based on the 80MHz bandwidth, introduces significant errors when applied to the 160MHz bandwidth. Specifically, when operating in the 5.8GHz band, data transmission is prone to interference from walls and obstacles, leading to less accurate reception of RSSI fingerprint data by users. Additionally, the current usage of the 5.8GHz spectrum is primarily dedicated to industrial Internet of Things (IoT), and the adoption of the indoor 5.8GHz band is not yet widespread. Consequently, there is a lack of suitable RSSI fingerprint datasets for research and positioning purposes. Therefore, accurately determining the indoor user position within the 160MHz bandwidth has emerged as a crucial research challenge in the FTTR WLAN scenario.

D. ORGANIZATION of CHAPTERS

The study is broken down into five chapters as follows:

Chapter 2 is dedicated to the literature review, which includes an introduction and a review of the different machine learning methods used for RSSI-Based ML, CSI-Based ML, and Channel Frequency Response. Chapter 3 describes the process of synthesizing the FTTR scene dataset. This chapter covers scene analysis, dissemination path, and the

DOI: 10.17148/IJARCCE.2024.131101

generation of Channel Frequency Response images. Chapter 4 is focused on FTTR scene location inversion, which includes PCA pre-processing based on parallel paths, DNN network training, and online position estimation and error analysis. This chapter provides a detailed explanation of the DNN network used for indoor positioning, the process of training the network, and the steps taken to estimate user location. Chapter 5 presents the results and analysis of the research work. This chapter includes scene setting, technical specifications, accuracy of estimation, convergence analysis, time complexity, and similarity analysis. Finally, Chapter 6 concludes the research work with a summary of the main findings and contributions of the study.

II. LITERATURE REVIEW

E. INTRODUCTION

This chapter provides a comprehensive overview of existing indoor positioning techniques, topologies, and technologies, along with their corresponding performance metrics, advantages, and disadvantages. The definitions necessary to understand indoor positioning systems are also presented. In particular, this section focuses on the utilization of machine learning (ML) and intelligent algorithms in indoor positioning systems based on various fingerprint signals. A comparative analysis is presented, which takes into account various factors such as location accuracy, energy consumption, complexity, and other relevant factors of diverse IPS. The main objective is to provide a comprehensive understanding of the performance of different localization systems, and to facilitate the selection of the most suitable IPS for specific applications. The analysis considers the latest research and development in the field of indoor positioning, and provides a critical evaluation of the strengths and limitations of different techniques and technologies.

F. RSSI-BASED ML

1. K-NEAREST NEIGHBOR:

K-Nearest Neighbor (KNN) is a supervised learning algorithm that is widely used in many fields, including indoor localization systems.The basic idea of KNN algorithm is to find the K training samples closest to the input samples in a dataset and use the information from these neighbors for classification or regression prediction. In indoor localization systems, the KNN algorithm performs location estimation by matching the collected RSSI signals with the data in the fingerprint database. The performance of the algorithm depends mainly on the selected K values and the corresponding distance metric.The KNN algorithm is simple to use and has good classification and regression performance at the same time.Computation of the signal distance to each fingerprint by utilizing:

$$d = \sqrt{\sum_{l=1}^{L} \left(RSSI_{m,l} - RSSI_{l} \right)^2} \tag{1}$$

Bahl et al.**Error! Reference source not found.** presented a pioneering work, named RADAR, which aimed to analyze the propagation model of wireless signals for indoor positioning and applied the KNN algorithm for the first time. They suggested that the average value of the K-nearest neighbor coordinates is closer to the actual location than a single neighbor. The experimental setting comprised of a floor area of 980 square meters with over 50 office rooms, and achieved an average localization error of 2-3 meters. This groundbreaking work paved the way for the application of machine learning algorithms in wireless indoor positioning, and established a solid foundation for subsequent research.

The K-nearest neighbor (KNN) algorithm is a popular technique for indoor positioning systems. However, the accuracy of estimated positions may significantly vary based on the chosen K value for the algorithm. Hence, when K is fixed, the estimation error of positions may not be further reduced. To address this challenge, Oh J et al.**Error! Reference source not found.** proposes an algorithm that adaptively adjusts the K value for each position by analyzing the correlation between the K value and the received WiFi signal strength. The proposed algorithm offers more than a 30% improvement in positioning accuracy compared to the traditional KNN algorithm with a fixed K value. This adaptive KNN algorithm can adjust the K value to account for the varying levels of signal strength, resulting in more accurate position estimation. The proposed algorithm has the potential to enhance the performance of indoor positioning systems, which can be useful in various applications that require high accuracy in location detection.

The utilization of Wi-Fi Received Signal Strength Indicator (RSSI) for indoor localization has gained widespread attention due to its ability to utilize the existing Wi-Fi infrastructure. However, the performance of such systems is often

DOI: 10.17148/IJARCCE.2024.131101

affected by challenges such as signal attenuation caused by multipath propagation and environmental changes. To address these challenges and enhance the accuracy of indoor localization, an improved Spearman-distance-based K-Nearest-Neighbor (KNN) scheme is proposed by Y. Xie**Error! Reference source not found.**. Simulation results indicate that the proposed approach outperforms the original KNN method in environments characterized by severe multipath fading and temporal dynamics. The improved KNN algorithm leverages the Spearman correlation coefficient to adaptively adjust the distance metric based on the statistical properties of the RSSI signal, which leads to improved localization accuracy. The results of this study are expected to provide valuable insights and guidance for the development of more robust indoor positioning systems that can better withstand the effects of multipath and environmental changes.

2. SUPPORT VECTOR MACHINE:

Support Vector Machine (SVM) is a machine learning method based on statistical theory that offers certain advantages in processing high-dimensional data and solving nonlinear problems. It is particularly useful in addressing the regression problem between fingerprints and positions in indoor positioning systems. SVM finds a hyperplane that maximizes the margin between two classes by transforming the original data to a higher-dimensional feature space. The decision boundary is determined by the support vectors, which are the closest points to the hyperplane.

Wu Z et al.**Error! Reference source not found.** presents a novel approach for indoor localization using the online independent support vector machine (OISVM) classification method and undersampling techniques. The proposed system utilizes the received signal strength indicator (RSSI) of Wi-Fi signals for location estimation. To address the imbalanced data problem associated with OISVM, a new undersampling algorithm is developed. Additionally, a kernel function parameter selection algorithm is introduced for the training process, resulting in significant reductions in both training and prediction time complexity. Experimental results demonstrate that the proposed method achieves a substantial improvement in training and prediction speed by at least ten and five times, respectively. Furthermore, the online learning feature leads to a reduction of 0.8 m in estimation error, making it an ideal solution for portable devices with limited processing power and memory. These findings highlight the potential of OISVM-based methods and undersampling techniques in improving the accuracy and efficiency of indoor localization systems.

C. Figuera**Error! Reference source not found.** proposes a novel technique that incorporates a priori information within the learning machine, utilizing the spectral information of the training set and a complex output to take advantage of cross information in two dimensions of location. Specifically, a SVM algorithm is modified to create three advanced methods that incorporate this information: one utilizing an autocorrelation kernel, another using a complex output, and a third combining both. Experimental results demonstrate that incorporating a priori information significantly improves location performance when compared to k-nn and a standard SVM with Gaussian kernel. Moreover, the proposed algorithms show reduced time complexity in both training and prediction processes, making them suitable for portable devices with limited processing power and memory. Overall, this technique represents a significant advancement in indoor positioning algorithms that rely on Wi-Fi signal strength measurements.

3. EXTREME LEARNING MACHINE:

The demand for location-based services in indoor environments has increased in recent years, leading to a significant research interest in fingerprint-based indoor localization. This method relies on received signal strength (RSS) measurements in wireless sensor networks, which are collected by a smartphone equipped with internal sensors. However, the accuracy of fingerprint localization heavily relies on the quality of feature extraction and classification algorithms. Khatab Z E at al.**Error! Reference source not found.** propose a novel algorithm that leverages deep learning, extreme learning machines, and high-level features extracted by autoencoder to improve the performance of both feature extraction and classification. In addition, we address the dynamic nature of the environment by gradually increasing the number of training data to update the fingerprint database. Simulation results demonstrate that our proposed method achieves a significant improvement in localization performance compared to existing methods. The use of high-level features extracted by autoencoder and increasing the number of training data contribute to the enhanced performance of our proposed algorithm. This method has the potential to significantly improve the accuracy and reliability of indoor localization for a range of applications.

Zou H at al.**Error! Reference source not found.** present a novel approach to address this issue by transforming the received signal strength (RSS) to a standardized location fingerprint using Procrustes analysis. We introduce a new similarity metric, called the signal tendency index (STI), to match standardized fingerprints. We analyze the capability of the proposed STI in handling device heterogeneity and environmental changes. We then integrate the strengths of both STI and weighted extreme learning machine (WELM) to develop a robust and precise IPS. Finally, we conduct extensive

DOI: 10.17148/IJARCCE.2024.131101

experiments to compare the performance of the proposed IPS with existing solutions. The results demonstrate that our IPS outperforms existing solutions in terms of its robustness to device heterogeneity.

Zou H at al.**Error! Reference source not found.** proposes an indoor localization algorithm based on an online sequential extreme learning machine (OS-ELM). OS-ELM offers a fast learning speed, which reduces the time and manpower costs for offline site survey. Its online sequential learning ability allows the proposed localization algorithm to adapt in a timely manner to environmental dynamics. To evaluate the performance of OS-ELM, experiments under specific environmental changes such as variations in occupancy distribution and events of opening or closing doors are conducted. The simulation and experimental results demonstrate that the proposed localization algorithm provides higher localization accuracy than traditional approaches, due to its fast adaptation to various environmental dynamics. The proposed algorithm has the potential to reduce the intensive costs of manpower and time for offline site survey and improve the flexibility of IPSs to environmental changes.

G. CSI-BASED ML

Wu et al. **Error! Reference source not found.** introduced a novel approach to indoor localization using channel state information (CSI) to establish a transmission model and designed a localization algorithm based on the frequency diversity of subcarriers in the orthogonal frequency-division multiplexing (OFDM) system. The proposed frequency-based indoor localization algorithm (FILA) was implemented on 802.11 network interface cards (NICs). The experimental results showed that the accuracy of the proposed method was significantly improved compared with traditional methods that rely on received signal strength indicators (RSSI). The FILA system can be regarded as a pioneer in the application of CSI to indoor localization, and this paper has played a significant role in providing a new research direction for indoor localization in recent years. The proposed approach not only addresses the limitations of RSSI-based methods, such as multipath and non-line-of-sight (NLOS) errors but also offers high accuracy and robustness against environmental changes. Therefore, the FILA system has contributed to the development of advanced indoor localization systems based on CSI. Yang et al. **Error! Reference source not found.** gave a detailed overview of the working principle of CSI signals in indoor localization, which was published in the same year, and made a careful comparison with the RSSI. This section summarizes and compares the existing indoor localization systems based on the CSI using ML algorithms.

Wang et al. proposed PhaseFi, an indoor localization fingerprint identification system that utilizes calibrated CSI phase information. In the offline stage, the authors designed a deep neural network with three hidden layers to train the calibrated phase data, and used weight to represent the fingerprint. To reduce computational complexity, a greedy learning algorithm was adopted to train the weights layer by layer, where the subnetwork between two successive layers constitutes a restricted Boltzmann machine (RBM). In the online phase, a probability method based on radial basis functions (RBFs) was used to estimate the position. Experimental results showed that the proposed method outperformed methods based on the RSSI in terms of localization performance. The PhaseFi system is a significant contribution to the field of indoor localization, as it utilizes CSI phase information and deep neural networks to achieve accurate localization, and provides a promising direction for future research. Wang et al. proposed the DeepFi indoor localization system, which is based on the calibrated CSI phase information. The system adopts a deep neural network, specifically a backpropagation neural network, to reduce the error of training the model and enhance the localization accuracy. Compared to existing algorithms, DeepFi exhibits significant advantages, and achieves the best accuracy of 0.95 m under two representative indoor environments. The deep neural network consists of multiple hidden layers, with each layer performing feature extraction and representation learning from the calibrated phase data. The output layer generates the location probability distribution based on the learned features. The system was evaluated on different indoor environments, including a multi-room office and a single-room laboratory, and compared with three existing algorithms. The experimental results showed that DeepFi outperformed the existing algorithms in terms of localization accuracy and robustness to environmental changes.

CSI **Error! Reference source not found.-Error! Reference source not found.** has become a popular choice for indoor localization due to its fine-grained information and temporal and spatial characteristics. However, it may not be suitable for large areas such as terminal buildings and requires careful consideration of its unique properties when designing localization algorithms. Intelligent localization methods, such as informative path planning based on reinforcement learning, can minimize the manpower and resources needed for data collection. To balance the cost in the offline stage and improvement in the online stage, researchers need to consider various factors, such as the informativeness of data and the distribution of fingerprint data in the target area. In conclusion, careful consideration of the characteristics of CSI and intelligent data collection methods are necessary for the development of accurate and efficient indoor localization algorithms**Error! Reference source not found.**.

DOI: 10.17148/IJARCCE.2024.131101

H. CHANNEL FREQUENCY RESPONSE

A channel frequency response (CFR) image is an image that reflects the amplitude, phase response, and other properties of a system or signal, using frequency as a parameter.CFR is often used to describe the transmission characteristics of a signal in a system and the effect of the system's transformation of the input signal.The CFR image is a fine-grained location-dependent metric that exhibits significant differences at different locations.

The channel frequency response (CFR) is a valuable location-specific information in WiFi systems that can be utilized for indoor positioning systems (IPSs). However, achieving centimeter-level accuracy in CFR-based IPSs using WiFi devices is challenging due to the limited bandwidth in WiFi systems. To overcome this limitation, Chen Chen at al.**Error! Reference source not found.** propose an IPS that leverages the spatial diversity in multiple-input-multiple-output (MIMO) WiFi systems, leading to a much larger effective bandwidth than the bandwidth of a single WiFi channel. The proposed IPS captures CFRs associated with locations-of-interest on multiple antenna links during the training phase. In the positioning phase, the IPS acquires instantaneous CFRs from a location to be estimated and compares them with the CFRs obtained in the training phase via the time-reversal resonating strength with residual synchronization errors compensated. The experiment results in an office environment demonstrate that, with a single pair of WiFi devices and an effective bandwidth of 321 MHz, the proposed IPS achieves detection rates of 99.91% and 100% with false alarm rates of 1.81% and 1.65% under the line-of-sight (LOS) and non-line-of-sight (NLOS) scenarios, respectively. Moreover, the proposed IPS is robust against environmental dynamics. The experiment results with a measurement resolution of 0.5 cm further demonstrate a localization accuracy of 1-2 cm in the NLOS scenario.

In the field of indoor positioning systems, it is crucial to accurately locate objects or people in dynamic environments. However, such environments often introduce variations in the channel frequency response (CFR), which complicates the localization process. Elmer R**Error! Reference source not found.** proposes a solution for dynamic indoor positioning based on CFR fingerprints. Experimental results show that the indoor fingerprints become uncorrelated within a 15-minute window, which necessitates frequent updates to the CFR database. To this end, three rapid CFR database updating methods are proposed, which enable accurate indoor localization even in the presence of environmental changes, such as human movement or interference from other wireless signals. Remarkably, the proposed solution achieves 100% localization accuracy for indoor locations that are separated by at least 5 cm, using only a single anchor node for estimation.

Tseng P at al.**Error! Reference source not found.** have implemented a channel sounder utilizing an orthogonal frequency-division multiplexing system to gather CIR measurements in both off-line and online modes. Furthermore, we have developed a ray-tracing (RT) channel predictor to acquire the primary attributes of the channel for the off-line predicted database. To our knowledge, we are the first to adopt RT as a channel predictor to facilitate indoor FP utilizing CIR measurements. We have employed coarse localization to categorize the reference points (RPs) based on the access point that provides the strongest RSS. We have proposed an RT-assisted FP (RAFP) method that estimates the position by merging the measured and predicted signatures to identify the RPs that exhibit the highest correlation values between the online measurement and the off-line measured and simulated CIR databases. The experimental results demonstrate that the RAFP-positioning with a hybrid of the predicted and measured CIR is capable of reducing the FP localization error by 25%. By integrating simulated CIRs, the RAFP offers the benefits of reduced human labor for off-line measurement collection and the usage of a reduced number of CIR measurements to sustain acceptable performance. The outcomes of our study encourage further development, which could entail cost-effective deployment by substituting the sounding system with wireless network interface cards.

III SYNTHESIS OF FTTR SCENE DATASET

I. INTRODUCTION

In conventional wireless networks, wireless devices adhere to the predetermined access protocols and primarily utilize the 2.4 GHz band for transmitting and exchanging data. However, in the FTTR WLAN scenario, the data transmission band is expanded to 160 MHz, which poses a challenge in the 5.8 GHz band as the transmission and bypassing ability for walls is compromised due to the shortened signal wavelength in this band range, being only half of the original 2.4 GHz band channel.Using the previous dataset for indoor positioning in such scenarios may result in significant errors. To address this issue, a suitable dataset for the 5.8 GHz band is necessary to ensure accurate indoor positioning in the FTTR WLAN scenario.

IJARCCE ISSN (O) 2278-1021, ISSN (P) 2319-5940

International Journal of Advanced Research in Computer and Communication Engineering

Impact Factor 8.102 ⁜ Peer-reviewed & Refereed journal ⁜ Vol. 13, Issue 11, November 2024

DOI: 10.17148/IJARCCE.2024.131101

Considering the newly introduced 80M available bands in the 5G band range in FTTR WLAN in contrast to traditional WLAN, the wavelength of the signal in this band range is only half of the original 2.4G band channel, which significantly weakens the transmission ability and bypassing capacity for walls. To synthesize a practical and effective dataset of FTTR WLAN scenarios, this study adopts the 802.11ax standard to simulate the reception process of wireless signals. To ensure the credibility and authenticity of the synthesized FTTR scene dataset, this study generates frequency response images of the test points in the frequency domain. In this regard, the wireless signal is subjected to a rigorous modeling process, followed by electromagnetic analysis through the utilization of the ray tracing technique to obtain the ray information of the measurement point. On this basis, the process of receiving wireless signals at the terminal is simulated.

J. SCENE ANALYSIS

Multi-bedroom gigabit broadband users in bathrooms, kitchens, bedrooms and other bedroom edges experience unstable Wi-Fi connections because the terminals are too far from the access point or the signal is constantly attenuated as it passes through walls. Therefore, when gigabit broadband service is delivered into the home over fiber, the assurance that every room is covered by a high-quality network and can accurately locate the user's position in the room is key to enhancing the user experience.

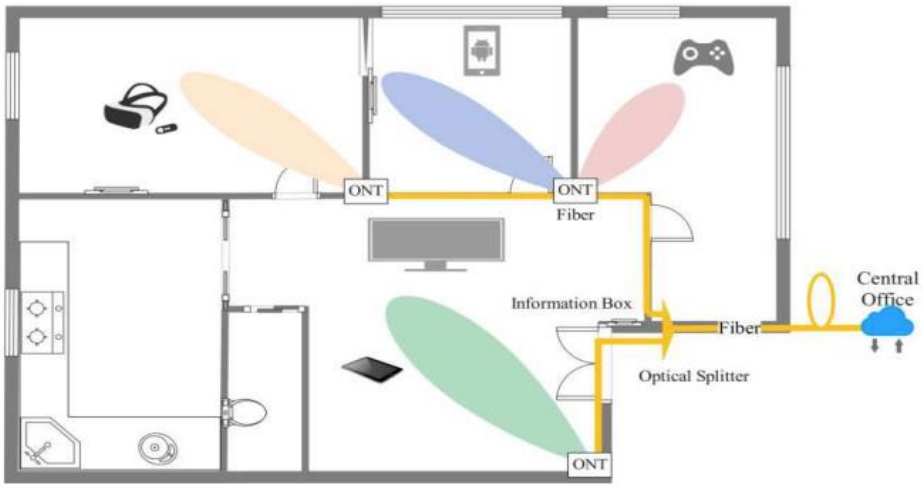

Figure 3.1 FTTR Scene diagram

This positioning technique analyzes the features from an observed scene. The scene can be any type of signal, from a sensor or from the environment itself that can be measured and used to differentiate between locations. Using this approach, the location of a device can be calculated based on the similarity between scenes. A WLAN fingerprinting positioning system is considered to be part of the scene analysis positioning technique and it is the foundation of the IPS presented in this thesis.

K. DISSEMINATION PATH

The use of channel prediction tools based on ray tracing techniques has the advantage of being efficient and cost-effective compared to traditional measurement-based methods. Furthermore, these tools can provide detailed and accurate channel information in complex environments where physical measurements may be difficult or impossible to obtain. In the field of wireless communication, channel prediction plays a crucial role in optimizing the performance of wireless networks. Ray tracing techniques have emerged as an effective tool for predicting wireless channel characteristics in complex indoor and outdoor environments.

By tracing the path of electromagnetic waves through the environment, channel information such as signal strength, delay spread, and angular spread can be predicted for each point in the scene. This information can then be used to optimize wireless network design, evaluate the performance of wireless communication systems, and develop advanced signal processing algorithms.As such, the use of ray tracing techniques in channel prediction has become an important area of research in the wireless communication industry, with many researchers and practitioners exploring novel approaches to

DOI: 10.17148/IJARCCE.2024.131101

improve the accuracy and efficiency of these techniques.

The ray-tracing model is the basic wireless signal transmission model, and to simplify the data synthesis process, the maximum reflection order of the wireless paths is set to 2 in the paper, i.e., only the direct and specular reflection paths of this model are considered simultaneously. This is because the contribution of diffraction and refraction paths to multipath superposition in indoor environments is much smaller than that of reflection paths.

Based on the ray-tracing model**Error! Reference source not found.** to describe the propagation path of the signal between the access point and the device terminal, the signal power received by the device terminal can be expressed as:

$$P^{3D}(d)=\frac{P_t\lambda^2}{(4\pi d)^2}\left|\sqrt{G_T(\phi_T,\theta_k)G_R(\phi_R,\theta_k)}\right. \times(\Gamma^{ceiling}(\theta_k))^{\lfloor\frac{k+1}{2}\rfloor}(\Gamma^{floor}(\theta_k))^{\lfloor\frac{k}{2}\rfloor}\left.\prod_{i=0}^{n}I_i(\theta_k)\right|^2 \tag{2}$$

$$\theta_k=\arctan\{\frac{2H[\frac{k+1}{2}]+(-1)^k h_2-h_1}{d}\} \tag{3}$$

where θ_k is the elevation angle of the kth ray, H,h_1,h_2 denotes the height of the building, transmitting antenna and receiving antenna, respectively; $G_T(\phi_T,\theta_k)$ and $G_R(\phi_R,\theta_k)$ are the gain of the transmitting and receiving antenna, respectively, ϕ_T and ϕ_R are the transmitting and receiving antenna angles, respectively; and the wavelength is λ. N reflected or transmitted from or through the wall between the transmitting antenna and the receiving antenna, the length of the propagation path is d, Γ and I are the reflection and interaction coefficients along the path, respectively, and $P^{3D}(d)$ denotes the received power along the path.

L. GENERATION of CHANNEL FREQUNCY RESPONSE IMAGE

The whole process of generating the reference signal for FTTR system, signal fading in multipath channel and CSI estimation at the terminal will be simulated next according to 802.11ax specification.

1. THE REFERENCE SIGNALS PRODUCED by ANALOG ACCESS POINTS:

The reference signal is the key signal designed for CSI measurement and received signal strength estimation in wireless communication. According to the 802.11ax protocol requirements of WiFi networks, the first segment of each data frame sent by the transmitter to the terminal contains the leading symbol, which completes a series of tasks such as channel estimation, time synchronization, and automatic gain control. At the same time, OFDMA technology is newly introduced to unify the time-frequency resources to be managed by the resource unit RU, and assign the RU the corresponding pilot frequency subcarriers for power adjustment and phase tracking. Thus the leading symbols are distributed on each subcarrier**Error! Reference source not found.**, and their signal form is expressed as:

$$s(t)=\sqrt{E_c}\sum_{k=1}^{L_bW}d_k\,p(t-kT_c-i_0T_c) \tag{4}$$

where E_c denotes the energy of each lead, W denotes the number of lead sequences, L_b denotes the lead sequence length, the pulse function $p(t)$ is normalized to unit energy, T_c denotes the duration, and the lead is assumed to start at the discrete time i_0.

IJARCCE ISSN (O) 2278-1021, ISSN (P) 2319-5940

International Journal of Advanced Research in Computer and Communication Engineering

Impact Factor 8.102 ⁜ Peer-reviewed & Refereed journal ⁜ Vol. 13, Issue 11, November 2024

DOI: 10.17148/IJARCCE.2024.131101

2. *ESTIMATION of CHANNEL FREQUNCY RESPONSE IMAGE at the TERMINAL:*

The following four operational steps are performed to obtain the spectrum response information using the leading signal emitted from the access point.

1) Considering direct radiation and reflection, the wireless transmission channel is modeled in the paper by superimposing the multipath components transmitted by ray tracing method :

$$h(\tau)=\sum_{n=1}^{N} a_n e^{-j\theta_n}\delta(\tau-\tau_n) \tag{5}$$

where a_n, θ_n, and τ_n are the amplitude, phase, and delay on the n th path, respectively; $\delta(\cdot)$ is the Dirac function; and N denotes the total number of paths in the environment. In addition, $h(t)$ is the channel impact response (CIR) of this multipath channel, which consists of the time delay multiplied by the amplitude and phase on the multiple paths. Thus, the received signal spectrum $R_s(f)$ can be expressed as the product of the transmit signal spectrum $T_s(f)$ and the channel frequency response $H(f)$, corresponding to the convolution of the two in the time domain. Since the calculation of the channel impulse response is very important, this paper estimates the channel by frequency multiplication followed by denoising using the Fourier inverse transform.

2) The received signal is demodulated by OFDM and corrected for the time offset, and the terminal obtains the received channel impulse response. The relative frequency impulse response matrix of all subcarriers can be represented in the form of a k -dimensional column vector :

$$H_r=(R_{Grid})_{k\times 1}/(ref_{Grid})_{k\times 1} \tag{6}$$

where k is the number of subcarriers, R_{Grid} denotes the channel frequency impulse response obtained from simulations in each subband, and ref_{Grid} denotes the channel frequency impulse response obtained from measurements in each subband.

3) For H_r, the information is transformed into the relative channel impulse response in the time domain using the Fourier inverse transform for noise reduction. Then, the relative channel impulse response after denoising can be expressed as :

$$H_n=\mathrm{F}^{-1}(H_r)W \tag{7}$$

where W is the time domain rising cosine window used for denoising, and $\mathrm{F}^{-1}(\cdot)$ denotes the Fourier inverse transform.

4) Finally, the frequency response image is obtained by Fourier transform H . As follows, $\mathrm{F}(\cdot)$ represents the Fourier transform :

$$H=\mathrm{F}(H_n) \tag{8}$$

IJARCCE ISSN (O) 2278-1021, ISSN (P) 2319-5940

International Journal of Advanced Research in Computer and Communication Engineering

Impact Factor 8.102 ⁜ Peer-reviewed & Refereed journal ⁜ Vol. 13, Issue 11, November 2024

DOI: 10.17148/IJARCCE.2024.131101

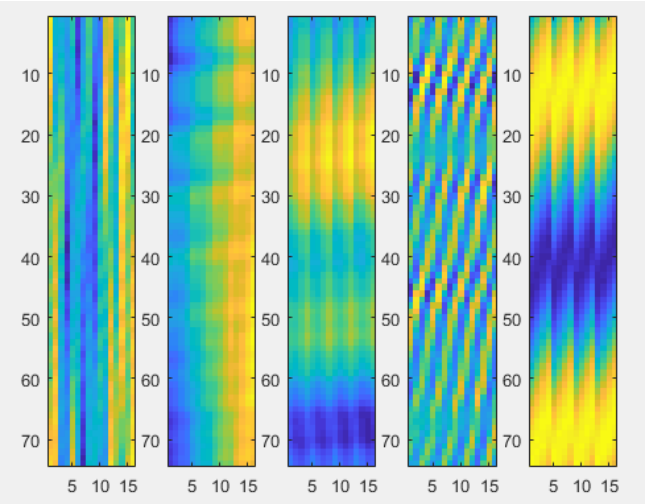

Figure 3.2 Frequency response image of a single terminal from 5 WiFi access points on the same floor at the test point

Throughout the terminal estimation process, the generated frequency response images are location-dependent and highly discriminative, as they reference the multipath propagation process of the leading symbols of the 802.11ax protocol. The 160M bandwidth available for FTTR WLAN is divided into 16 independent 10M bands, each independent band is used as a channel, and the wavelength corresponding to the center frequency of each band is used to estimate the propagation path. Also FTTR WLAN assigns a total of 76 groups of subcarrier schemes, each of which may be used as leading symbols and assigned guide frequency signals, so that each frequency response image is a 76 × 16 image. each column of pixels in the CFR image corresponds to a channel, while the width corresponds to the number of channels, and the physical significance of the CFR image is mainly focused on the frequency direction (vertical direction). Figure 3.2 shows the frequency response images of the signals received by a terminal device at five WiFi access points at different locations on the same floor. All the observed frequency response images obtained show good resolution, indicating that the frequency response image based method has high localization accuracy.

FTTR scene location inversion

M. INTRODUCTION

Position inversion, also known as localization, is an essential function for many location-based services and applications. It involves the use of measurements such as signal strength, time of arrival, and angle of arrival to infer the position of a mobile device. To achieve accurate localization, a two-step approach is commonly used, consisting of a preprocessing part and an online localization part.

In the preprocessing part, rich localization features are extracted from the received signals to provide a suitable input to the online localization algorithm. Multi-path transmission is common in wireless communications, and therefore, different convolutional kernels are designed to extract features from each path. This enables each path to independently determine a suitable feature extraction range, leading to diverse features that can be combined for accurate localization.

Additionally, feature extraction by principal component analysis (PCA) is performed to reduce the amount of data to be processed and maintain fast convergence. This is particularly important for real-time applications that require efficient and fast localization of mobile terminal devices. The online localization part then uses the extracted features to learn the relationship between the features and the terminal's position and estimate its location in real-time.

N. PCA PRE-PROCESSING BASED on PARALLEL PATHS

In the pre-processing stage, it is necessary to ensure the diversity of feature extraction first. Because the richer the extracted features are, the better it is for DNN to improve the localization accuracy in the localization process. Therefore, three parallel paths with different structures are used to extract different ranges of features. In this way, a single input frequency response image can produce different scales of output features by convolutional kernels of different sizes. Specifically a 1×1 filter, a 3×3 filter and a pair of 5×1+1×3 filters are used on each of the 3 parallel paths. This parallel

IJARCCE ISSN (O) 2278-1021, ISSN (P) 2319-5940

International Journal of Advanced Research in Computer and Communication Engineering

Impact Factor 8.102 ⁜ Peer-reviewed & Refereed journal ⁜ Vol. 13, Issue 11, November 2024

DOI: 10.17148/IJARCCE.2024.131101

path gives the image the ability to automatically select the appropriately sized convolution kernel for feature extraction. The smaller filter can effectively preserve the original frequency response image information, while the larger filter can more effectively capture the channel differences between adjacent subcarriers, thus revealing the location-dependent features implied between the subcarriers. n×1 and 1×n filters can better focus on the features of the frequency response image between subcarriers and between the pilot signals.

Specifically, if the input filter is a 76 × 16 CFR image, the r th row c th column matrix element corresponds to a pixel value of $f(r,c)$. After the filter of $m\times n$, the value of each pixel of the CFR image is replaced by the weighted average of the pixel values in the neighborhood around that pixel, and the weight is calculated by a Gaussian function. After the filtering the r th row c th column matrix element $f'(r,c)$ can be expressed as :

$$f'(r,c)=\frac{1}{2\pi\sigma^2}\sum_{i=-\frac{m-1}{2}}^{\frac{m-1}{2}}\sum_{j=-\frac{n-1}{2}}^{\frac{n-1}{2}}f(r+i,c+j)e^{-\frac{i^2+j^2}{2\sigma^2}} \tag{9}$$

where σ is the standard deviation of the Gaussian function.

At the same time, in order to reduce the amount of data for DNN training, the output of convolutional kernels of different paths is processed by PCA dimensionality reduction in the paper to speed up convergence while effectively extracting image features. the process of PCA dimensionality reduction includes the following four steps:

1) First, the mean value corresponding to each channel in the CFR image after multipath processing is set to 0. The purpose is to prevent large variables from dominating the principal components. That is, the mean value of each channel of the CFR image H of size $N_s\times N_p$ is obtained, denoted as: $A_{1\times N_p}$, where N_s denotes the number of subcarriers and N_p denotes the number of channels. and let the value of each carrier for each channel be subtracted from the mean to obtain the result H' :

$$H'_{i\times j}=H_{i\times j}-A_{1\times j}, i=1,\ldots,N_s, j=1,\ldots,N_p \tag{10}$$

2) Solve the feature covariance matrix S for the CFR image matrix H' after processing:

$$S=\frac{1}{N_p-1}\sum_{j=1}^{N_p}H'_{N_s\times N_p}(H'_{N_s\times N_p})^T \tag{11}$$

3) Based on the obtained eigencovariance matrix S , solve for the eigenvalues and eigenvectors, and arrange the eigenvalues in descending order, i.e. $\lambda_1\geq\lambda_2\geq\cdots\geq\lambda_k$. Arrange the eigenvectors corresponding to each eigenvalue in the form of a matrix, as:

$$\Lambda=\left(\vec{\xi}_1,\vec{\xi}_2,\cdots,\vec{\xi}_k\right) \tag{12}$$

4) The first N vectors from the feature vectors are selected as principal components, and the final matrix after dimensionality reduction is obtained as:

$$H_{N\times N_p}=\left(\vec{\xi}_1,\vec{\xi}_2,\cdots,\vec{\xi}_N\right)\cdot H'_{N_s\times N_p} \tag{13}$$

IJARCCE ISSN (O) 2278-1021, ISSN (P) 2319-5940

International Journal of Advanced Research in Computer and Communication Engineering

Impact Factor 8.102 ⁜ Peer-reviewed & Refereed journal ⁜ Vol. 13, Issue 11, November 2024

DOI: 10.17148/IJARCCE.2024.131101

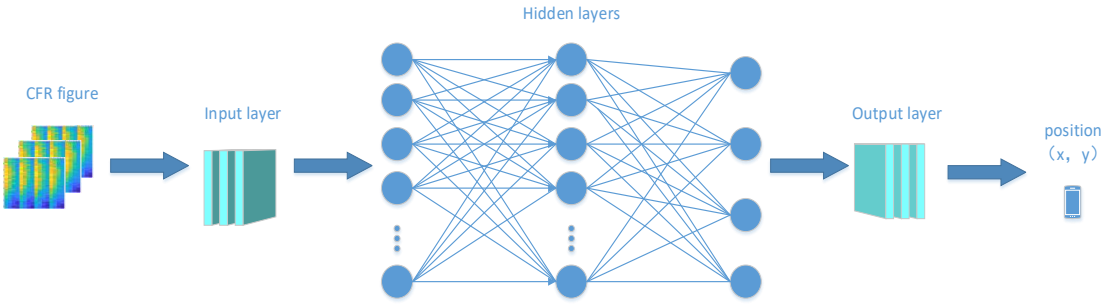

Figure 4.1 DNN network diagram

It is worth noting that in many previous works, PCA methods have been employed to process Received Signal Strength Indication (RSSI) datasets**Error! Reference source not found.Error! Reference source not found.**. In this study, PCA is employed to process images that have undergone parallel path filtering. This approach is advantageous as it can significantly reduce the dimensionality of the data and mitigate the overfitting issue by eliminating redundant features. Furthermore, PCA effectively reduces the amount of data while preserving the majority of the important information, thus enhancing the operation speed of the algorithm and reducing the memory space required for storing the data. In particular, the proposed method utilizes PCA to process images after parallel path filtering, which is beneficial in preserving the essential data information while reducing the computational and storage requirements. This feature is particularly important in the deployment of the algorithm in mobile terminal devices.

O. DNN NETWORK TRAINING

The matrices after the PCA dimensionality reduction process will be input to the DNN network**Error! Reference source not found.Error! Reference source not found.** for training the weight matrix W and bias matrix B in the network. The DNN network in this paper is shown in Figure 4.1 and contains one input layer, three hidden layers, and one output layer. Each hidden layer input and output contains 16 channels, so the weight and bias matrices that can be processed are 3 groups, both of size 16 × 16, $W_1 \sim W_3$ and $B_1 \sim B_3$ respectively. The output layer input contains 16 channels, and the output is an estimate of position $\hat{P} = (\hat{x}, \hat{y})$, whose corresponding weight matrix W_4 and bias matrix B_4 are of size 16 × 2. The data processing process using DNN networks involves two processes for the transfer of features of matrix data between each two layers.

1) The intermediate values are first obtained from the weight vector and bias vector between the input and output. For input x_i of the i channel, it is processed by the weight matrix W_k and bias matrix B_k weights of the k layer. The resulting intermediate value z_j for the j th channel can be expressed as:

$$z_j = \sum_{j=1}^{16} \left(w_{i,j} x_i + b_{i,j} \right) \tag{14}$$

where $w_{i,j}$ denotes the coefficient of linear relationship between the i th input and the j th output of the weight matrix W_k and $b_{i,j}$ denotes the bias between the i th input and the j th output of the bias matrix B_k.

2) The resulting intermediate values are then passed through an activation function to obtain the output. The activation function used in this paper is the tanh function, whose expression is: $\tanh x = \dfrac{e^x - e^{-x}}{e^x + e^{-x}}$. Thus the result of the next layer can be obtained as:

DOI: 10.17148/IJARCCE.2024.131101

$$f\left(z_j\right)=\tanh z_j=\frac{e^{z}-e^{-z}}{e^{z}+e^{-z}}=\frac{e^{\sum_{j=1}^{16}\left(w_{i,j}x_i+b_{i,j}\right)}-e^{-\sum_{j=1}^{16}\left(w_{i,j}x_i+b_{i,j}\right)}}{e^{\sum_{j=1}^{16}\left(w_{i,j}x_i+b_{i,j}\right)}+e^{-\sum_{j=1}^{16}\left(w_{i,j}x_i+b_{i,j}\right)}} \tag{15}$$

Let $f\left(\vec{x}\right)=\tanh\left(W\cdot\vec{x}+B\right)$, be the function after the processing of Eq. (14), then the final estimate of the user location coordinates obtained after the processing of three hidden layers and one output layer of the DNN network is:

$$\hat{P}=W_4\tanh\left(W_3\tanh(W_2\tanh(W_1H+B_1)+B_2)+B_3\right)+B_4 \tag{16}$$

During the training process of DNN networks, there are often errors between the estimated and actual values of user location coordinates, and a single calculation by pre-set weight vector and bias vector calculation does not result in a correct location estimate, so a correction of the DNN network weight vector and bias vector is also required. This process is usually performed by back propagation method. Specifically, the output error of a DNN network is usually measured by the loss function. The loss function characterizes the difference between the predicted output of the model and the actual labels, and is usually used to measure the accuracy of the model.

In this paper, the mean square error function is chosen as the loss function, denoted as C_{reg} , whose expression is:

$$C_{reg}=\frac{1}{N}\sum_{i=1}^{N}(P-\hat{P})^2 \tag{17}$$

where z denotes the actual user location coordinates. And the linear correlation coefficients w_i and b_i are corrected by back propagation using gradient descent method, which is modified as: $w_i'=w_i-\frac{\partial C_{reg}}{\partial w_i}\cdot\alpha$ and $b_i'=b_i-\frac{\partial C_{reg}}{\partial b_i}\cdot\alpha$, where α denotes the iteration step. Forward and backward propagation are performed in each iteration until the target loss function converges. In the forward propagation phase, each hidden layer calculates the output by adding deviations to the weighted inputs and passing the results to the activation function. The data flows from the input layer to the output layer to get the prediction results, and the output of each hidden layer is used as the input to the next hidden layer. In the backpropagation phase, the error is propagated in the opposite direction from the output layer to the input layer to calculate the gradient of the loss function with respect to the model parameters. The error term in the output layer is calculated as the difference between the actual output and the desired output, and the error term in each hidden layer is calculated as a weighted sum of the errors in the next layer. After repeated iterations as in Eq. (17) and back propagation, the iterations are stopped until the maximum number of iterations is reached or the change in the weights is less than the iteration threshold. The trained weight vector and bias vector are used as parameters of the DNN network for subsequent online position estimation. In this paper, the learning rate in the model is set to 1e-3, the number of iterations is 400, and the canonical weight is 0.1 to improve the accuracy of the subsequent online position estimation.

From the whole mathematical process of training and localization, localization by channel frequency response images adds two advantages over the traditional method of using RSSI for localization.

1) During the generation of channel frequency response (CFR) images, this paper proposes a method that considers the influence of the relationship between transmit power and receive power at different angles. In contrast to previous methods that rely solely on measured power information in RSSI datasets, this approach accounts for the effects of direct and primary reflection, thereby enabling the inclusion of multiple spatial angle paths beyond those present in the original RSSI method based on theoretical formulae. Additionally, this method incorporates more sampling data than traditional RSSI techniques in the input of data sampling points.

IJARCCE ISSN (O) 2278-1021, ISSN (P) 2319-5940

International Journal of Advanced Research in Computer and Communication Engineering

Impact Factor 8.102 ⁜ Peer-reviewed & Refereed journal ⁜ Vol. 13, Issue 11, November 2024

DOI: 10.17148/IJARCCE.2024.131101

2) In the training phase for measuring point localization, this paper employs a deep neural network (DNN) comprising four layers of weights and biases. Compared to the 1D inversion method, the DNN model is capable of training four times the number of weight vectors relative to the input matrix. Moreover, the DNN model obtains the final output estimate by processing the original input function through the weight matrix and bias matrix multiple times, which can be viewed as a nonlinear transformation in nature. Consequently, the DNN model is able to achieve a more accurate and closer fit than the one-dimensional inversion method.

P. ONLINE POSITION ESTIMATION and ERROR ANALYSIS

The aim of fine localization is to find an optimal position regression expression for the final position calculation, therefore DNN networks are used for position estimation. This is due to the ability of DNN neural networks to provide multilayer nonlinear transformations according to the activation function and to have special advantages. On the one hand the relationship between frequency response images and position points is complex, and considering the powerful nonlinear fitting capability of DNN, the choice of DNN network can guarantee the accuracy of position inversion. On the other hand, DNN has powerful feature extraction capability, which can extract location-related features from frequency response images and convert them into higher-level abstract representations, which helps the proposed localization method to be smoothly transposed under different scene conditions.

The following section describes the processing flow of the user location calculation and analyzes the errors that may form using this location estimation method.

1. USER LOCATION CALCULATION:

In the phase of calculating the user's location, the path transfer function of the signal can be calculated by the user's transmit power and the RSSI value measured at the receiving point H_m. If the user's transmit power at the measuring point is $P_{t,m}$ and the RSSI information at the receiving point is $P_{r,m}$, then the path transfer function of the signal is $H_m = P_{r,m} / P_{t,m}$.

The path transfer function H_m is Fourier transformed, i.e.:

$$H = \mathrm{F}(H_m) \tag{18}$$

The obtained Fourier transform results are likewise assigned to the 16 10M independent frequency bands used by the FTTR WLAN as 16 channels. And the intensity of the frequency domain transfer function is calculated according to the 76-group subcarrier scheme assigned to the FTTR WLAN to obtain the 76 × 16 CFR image corresponding to the measured values.

After the 76×16 CFR image is processed by parallel path filtering and PCA feature extraction as shown in Figure 4.2, the processed CFR image is obtained . The image is fed into a DNN network with adjusted weights to estimate the position, i.e., the image is fed into the input layer of the DNN network and processed by the weights in the DNN network. Only the forward propagation process of the data is performed in the location estimation process, as shown in Equation (15), and the output of the DNN network is the predicted user location.

2. ERROR ANALYSIS:

In order to evaluate the localization accuracy of this algorithm, the commonly used average error **Error! Reference source not found.Error! Reference source not found.**(Err_{mean}) is used in the paper. The average error is defined as follows:

$$Err_{mean} = \frac{1}{N_{ue}} \sum_{i=1}^{N_{ue}} \| P_i - \hat{P}_i \|_2 \tag{19}$$

IJARCCE ISSN (O) 2278-1021, ISSN (P) 2319-5940

International Journal of Advanced Research in Computer and Communication Engineering

Impact Factor 8.102 ⁜ Peer-reviewed & Refereed journal ⁜ Vol. 13, Issue 11, November 2024

DOI: 10.17148/IJARCCE.2024.131101

Where $\hat{P}_i = (\hat{x}_i, \hat{y}_i)$ is the estimated position of the i th terminal, $P_i = (x_i, y_i)$ is the actual position of the i th terminal, N_{ue} is the number of terminals, and $\|\cdot\|_2$ is the Euclidean distance. The error between the estimated position coordinates of the i th terminal and the real position coordinates of the measurement point can be calculated as follows:

$$\| P_i - \hat{P}_i \|_2 = \| P_i - W_4 \tanh\left(W_3 \tanh(W_2 \tanh(W_1 H_i + B_1) + B_2) + B_3\right) - B_4 \|_2 \quad (20)$$

where H_i denotes the processed CFR image converted from the RSSI value measured at the i th terminal.

The error of the proposed algorithm in this paper contains the error generated when training the DNN network weight matrix and bias matrix using the dataset and the error generated when using the processed CFR images for position estimation, i.e., training error and inversion error. The source of training error has several components, 1) the error formed when analyzing the multipath effect when obtaining the signal strength at the access point ε_1, 2) the error generated by truncating the Fourier transform and Fourier inverse transform of the spectrum when generating the channel frequency response (CFR) image ε_2. 3) the truncation error generated when performing the PCA processing of the CFR image ε_3 . Therefore, the error formed during the training phase E_r can be expressed as:

$$E_r = \sqrt{\varepsilon_1^2 + \varepsilon_2^2 + \varepsilon_3^2} \quad (21)$$

The relative error $\varepsilon_1^2 = \Delta d / d$ formed by the multipath effect when the signal strength is obtained at the access point . where d denotes the distance between the measurement point and the receiving point, and Δd denotes the maximum distance difference between the paths formed due to the multipath effect.

Channel frequency response (CFR) image generation, truncated spectrum of the Fourier transform and Fourier inverse transform error: assume that the Fourier transform of the signal is $H(\omega)$, truncated spectrum of the Fourier transform is $H'(\omega)$, truncated frequency domain of the range: $(-N\Delta\omega, N\Delta\omega)$, then the error can be obtained: $\Delta H(\omega) = H(\omega) - H'(\omega)$, through the Parseval theorem can be obtained: $\varepsilon_2^2 = \frac{1}{2\pi}\int_{-N\Delta\omega}^{N\Delta\omega} |\Delta H(\omega)|^2 \, d\omega$.

In the process of position estimation, the truncation error generated by PCA processing of CFR images is: $\varepsilon_3{}^2 = \frac{1}{M}\sum_{i=1}^{M} \| n_i - \hat{n}_i \|^2$, where M denotes the number of data samples, n_i denotes the i th sample of the original data, and $\hat{n}_i$ denotes the reconstruction result of this sample after PCA dimensionality reduction, i.e., the data matrix obtained by PCA dimensionality reduction and then recovery.

(4) The estimation error formed by the weights and biases of each layer during the training process of the DNN network.

From the above expression, it is clear that the error value of Err comes from the influence of W and B weight matrices of each layer. The W and B weight matrices of each layer are corrected by the gradient descent algorithm, so the W and B weight matrices are ultimately determined by the iteration thresholds $w_{\max}$ and $b_{\max}$ in the gradient descent algorithm. When the iteration threshold is smaller, it indicates that $w_i' - w_i$ and $b_i' - b_i$ are smaller, i.e., the smaller $\frac{\partial C_{reg}}{\partial w_i} \cdot \alpha$ and $\frac{\partial C_{reg}}{\partial b_i} \cdot \alpha$. Therefore, the smaller the loss function C_{reg} is, the more accurate the predicted position coordinates are to the actual position coordinates, and the smaller the error is. Assuming that the

IJARCCE ISSN (O) 2278-1021, ISSN (P) 2319-5940

International Journal of Advanced Research in Computer and Communication Engineering

Impact Factor 8.102 ⁜ Peer-reviewed & Refereed journal ⁜ Vol. 13, Issue 11, November 2024

DOI: 10.17148/IJARCCE.2024.131101

iteration thresholds of the whole DNN network are set to W_T and B_T, the final error size of the position estimation is obtained as :

$$\| P_i - \hat{P}_i \|_2 = W_T \tanh\left(W_T \tanh(W_T \tanh(W_T E_r + B_T) + B_T) + B_T\right) + B_T \tag{22}$$

Considering that the activation function of the hidden layer neurons in the DNN network in this paper uses the tanh function, whose expression is $\tanh x = \frac{e^x - e^{-x}}{e^x + e^{-x}}$. It is not difficult to obtain after expanding e^x Taylor that when x is small there are:

$$\tanh x \approx x + \mathrm{O}\left(x^3\right) \tag{23}$$

Therefore, the error formed by each hidden layer $\tanh(W_T E_r + B_T) \approx W_T E_r + B_T$, i.e., each hidden layer does not amplify the error, so the error formed by the whole DNN network is less than $\left(W_T E_r + B_T\right)^4$.

The flow of the whole algorithm is shown in Figure 4.2. In the FTTR synthesis data set generation part, the 802.11ax compliant guide frequency signal is modulated and input to the ray path model at the corresponding location, and then the frequency response image is formed through the receive link. In the position estimation pre-processing stage the features of the frequency response image are first extracted by parallel path, and PCA dimensionality reduction processing reduces the data to be processed. In the position inversion stage, the model parameters for position estimation are trained by DNN network, and the measured RSSI is used to estimate the position information by the model parameters.

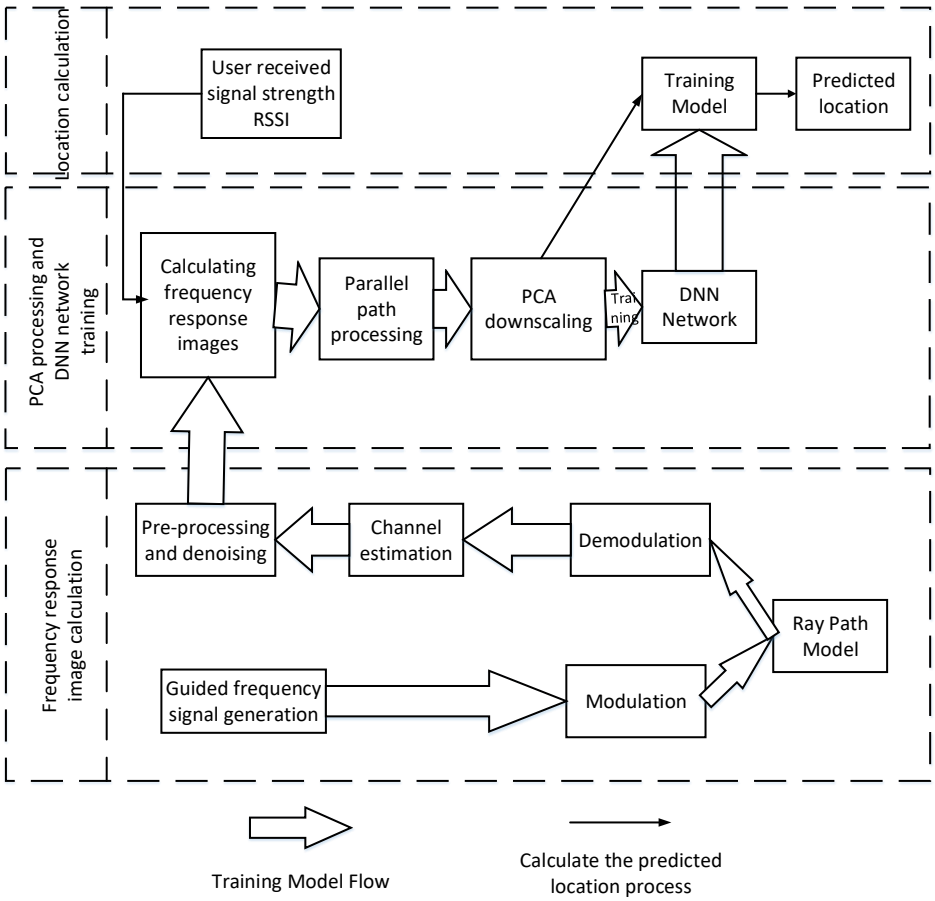

IJARCCE ISSN (O) 2278-1021, ISSN (P) 2319-5940

International Journal of Advanced Research in Computer and Communication Engineering

Impact Factor 8.102 ⁜ Peer-reviewed & Refereed journal ⁜ Vol. 13, Issue 11, November 2024

DOI: 10.17148/IJARCCE.2024.131101

Figure 4.2 Flow chart of indoor positioning of FTTR scenes

The proposed method and the traditional DNN network both include input, hidden and output layers, and the output of each neuron is used as the input of the next layer, and the weights and biases are optimized by the back propagation algorithm to minimize the loss function. However, the method in this paper differs from traditional DNN networks in that the dimensionality of the data is reduced and a large number of features are retained by PCA dimensionality reduction. In addition, the activation function used in the hidden layer is tanh function, which is smoother, easier to derive and faster to converge than the traditional DNN network using sigmoid function. In this paper, compared with the convolutional neural network (CNN), both of them can process a large amount of data and learn the mapping relationship between input and output from it. However, CNN networks use convolutional kernels to extract feature information from images, while the method in this paper has no explicit processing structure and generally contains multiple layers of fully connected layers. In addition, the algorithm proposed in this paper has strong nonlinear fitting ability and is trained by an optimization function with high generalization ability. Moreover, the data in this paper are generated based on the electromagnetic wave propagation principle, which retains certain transmission characteristics and has certain adaptability.

IJARCCE ISSN (O) 2278-1021, ISSN (P) 2319-5940

International Journal of Advanced Research in Computer and Communication Engineering

Impact Factor 8.102 ⁜ Peer-reviewed & Refereed journal ⁜ Vol. 13, Issue 11, November 2024

DOI: 10.17148/IJARCCE.2024.131101

RESULTS AND ANALYSIS

Q. *SCENE SETTING*

A three-story building with floors measuring 51 m by 28 m was used to collect the data. The dataset**Error! Reference source not found.** only covers roughly 50% of building extents due to some locational restrictions. With an 80 MHz bandwidth and 5 W of broadcast power, the WiFi access point operates at 2.4 GHz. The building's floor plans are seen in Figure 5. Each measurement was taken at a distinct absolute place, as shown in the graphic below by the location points marked in red. The black dots, which are anchored at a height of 2.5 meters above the floor, indicate the positions of WiFi connection points on the first and second levels. In order to avoid coplanarity, the simulation used a random floating height of 0.1m. The client for positioning the user is a Samsung Galaxy Younggt-S5360 smartphone.

Each measurement in the collection, which has 1,571 records and 65 features, contains data about the measurement's precise location, RSSI readings, time stamps, and possibly some IDs. The measurement component also contains information gathered from the magnetometer, WLAN card, and Bluetooth interface. A genuine three-dimensional vector is the magnetometer's output. WiFi RSSI values vary from 11 to 42, each location has a matching access point with a value between [-96, -34], and if no signal strength is detected, the value is set to Null. In this study, 32 columns of data ranging in size from 11 to 42 columns are used to calculate the frequency response using the picture computation method described above using the signal strength characteristic determined by AP. The related ray tracking model is also computed using the relative position coordinates of users measured in the data set and the position coordinates of AP.

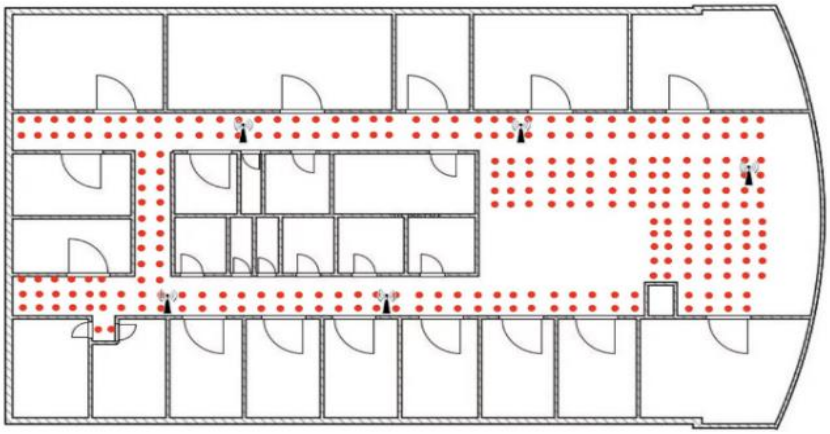

Figure 5. 1 Location of the measurement point and access point on the first floor.

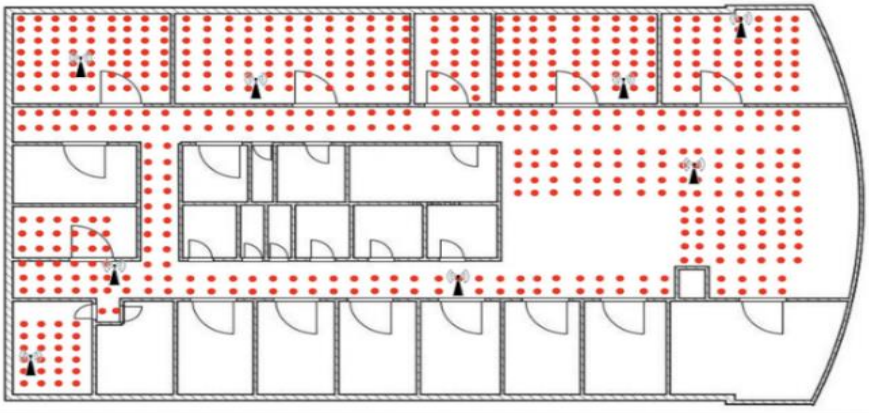

Figure 5. 2 Location of the measurement point and access point on the second floor.

IJARCCE ISSN (O) 2278-1021, ISSN (P) 2319-5940

International Journal of Advanced Research in Computer and Communication Engineering

Impact Factor 8.102 ⁜ Peer-reviewed & Refereed journal ⁜ Vol. 13, Issue 11, November 2024

DOI: 10.17148/IJARCCE.2024.131101

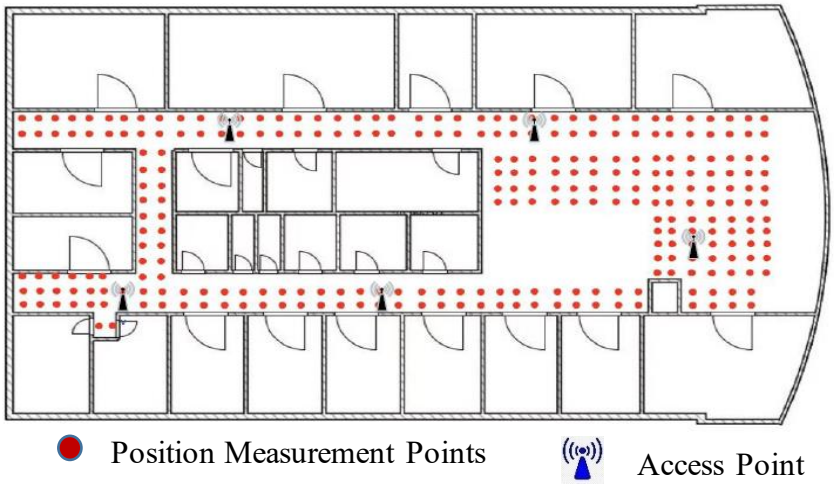

Figure 5. 3 Location ofhe measurement point and access point on the third floor.

R. TECHNICAL SPECIFICATIONS

In this research, Err_{mean} is employed to assess the positioning performance of this method. The following definition applies to the mean error:

$$Err_{mean} = \frac{1}{N_{ue}} \sum_{i=1}^{N_{ue}} \| P_i - \bar{P}_i \|_2 \tag{24}$$

Among them, the $\bar{P}_i$ for the estimates of the i th a terminal location, P_i for the actual location of the i th terminal, N_{ue} for the number of terminals, $\| \cdot \|_2$ is the Euclidean distance.

In addition, since this paper uses the existing WiFi fingerprint data set to synthesize the FTTR scene data set, the consistency between the synthesized data set and the obtained data set needs to be evaluated. Structural similarity index (SSIM)**Error! Reference source not found.Error! Reference source not found.** is one of the commonly used indicators to compare image quality, and its value ranges from 0 to 1, representing the structural similarity between the original image and the reconstructed image. Specifically, SSIM measures similarity in terms of brightness, contrast, and structure. Therefore, SSIM is used to evaluate the generated CFR image and the corresponding sampled CFR image. SSIM is defined as follows:

$$SSIM(m,n) = \frac{(2\mu_m\mu_n + C_1)(2\sigma_{mn} + C_2)}{(\mu_m^{\ 2} + \mu_n^{\ 2} + C_1)(\sigma_m^{\ 2} + \sigma_n^{\ 2} + C_2)} \tag{25}$$

$$\mu_m = \frac{1}{N} \sum_{i=1}^{N} m_i \tag{26}$$

The m and n is used to compare two nonnegative image signal, μ_m is the average brightness. The square root of the variance is used as an estimate of the signal contrast by:

$$\sigma_m = \left(\frac{1}{N-1} \sum_{i=1}^{N} (m_i - \mu_m)^2\right)^{\frac{1}{2}} \tag{27}$$

IJARCCE ISSN (O) 2278-1021, ISSN (P) 2319-5940

International Journal of Advanced Research in Computer and Communication Engineering

Impact Factor 8.102 ⁜ Peer-reviewed & Refereed journal ⁜ Vol. 13, Issue 11, November 2024

DOI: 10.17148/IJARCCE.2024.131101

$$\sigma_{mn} = \frac{1}{N-1}\sum_{i=1}^{N}(m_i - \mu_m)(n_i - \mu_n) \tag{28}$$

S. *ACCURACY of ESTIMATION*

The first and second floors of the building's measurement data from the data set in the literature are utilized as training samples to train the DNN network in the proposed technique, which is then used to test the positioning performance. Additionally, the DNN network's model parameters are used to forecast where the measuring points will be on the building's third floor. The training sample contains 1000 points, while the projected position of the measuring points contains 500 points. The cumulative distribution function of distance error of the 500 measuring points is shown in Figure 5. As a comparison algorithm**Error! Reference source not found.**, reference adopts Weighted k-Nearest Neighbor (WKNN) and Long Short-Term Memor (LSTM) in the data set of reference. The parameters of k in WKNN algorithm are adjusted (k= 13,21,35) The average distance errors estimated under different conditions are obtained. Therefore, the WKNN-LSTM method adopted in literature is used as a comparison scheme in this paper, and the cumulative distribution function of distance error obtained by this scheme is shown in Figure 5.4.

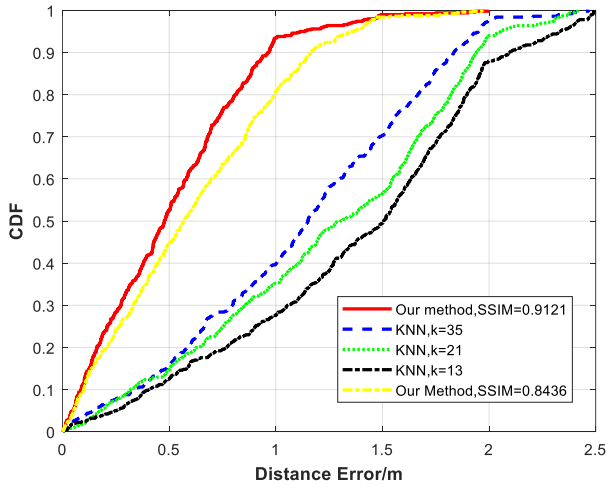

(1) The first floor

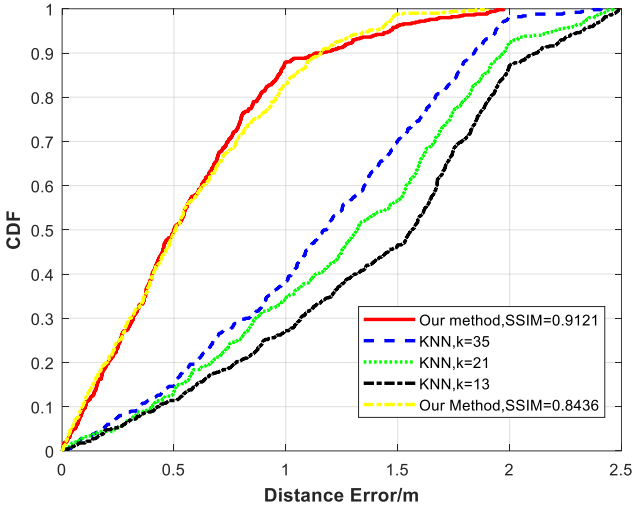

(2) The second floor

Figure 5.4 Cumulative distribution function of distance error

According to the results observed in Figure 5.4 the position estimation errors of the method proposed in this research are all smaller than those of the WKNN-LSTM method for the observation points in this data set. According to the cumulative distribution function of distance error, the method proposed in this paper can be calculated in The average error of position

IJARCCE ISSN (O) 2278-1021, ISSN (P) 2319-5940

International Journal of Advanced Research in Computer and Communication Engineering

Impact Factor 8.102 ⁜ Peer-reviewed & Refereed journal ⁜ Vol. 13, Issue 11, November 2024

DOI: 10.17148/IJARCCE.2024.131101

estimation is 0.86 m, that of comparison WKNN-LSTM (k=13) method is 1.83 m, that of WKNN-LSTM (k=21) method is 1.79 m, that of WKNN-LSTM (k=35) method is 1.72 m. Therefore, the position estimation accuracy of the proposed method is better than that of WKNN-LSTM, and the position estimation error can be less than 0.9m, thus achieving fine-grained position estimation. When the distance error is equal, the cumulative distribution function becomes larger with the increase of the SSIM value. In the case of distance error of 1 meter, when the SSIM value increases from 0.8436 to 0.9121, the cumulative distribution function of distance error will increase by 0.1.That is, there are more position points less than 1 meter distance error, so the positioning accuracy is higher and the average error is smaller.

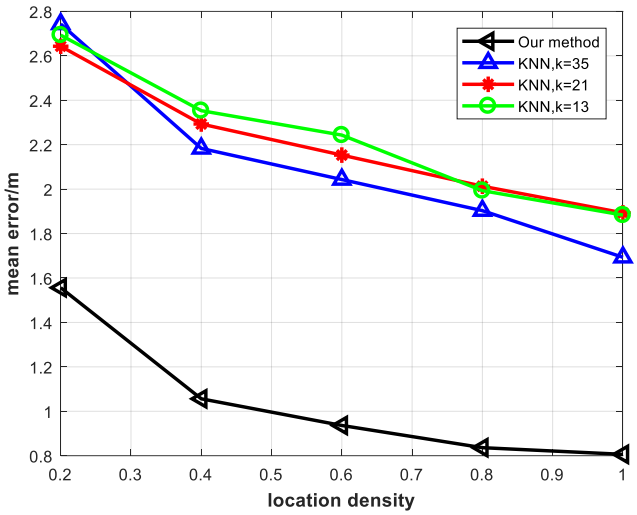

(a) The first floor

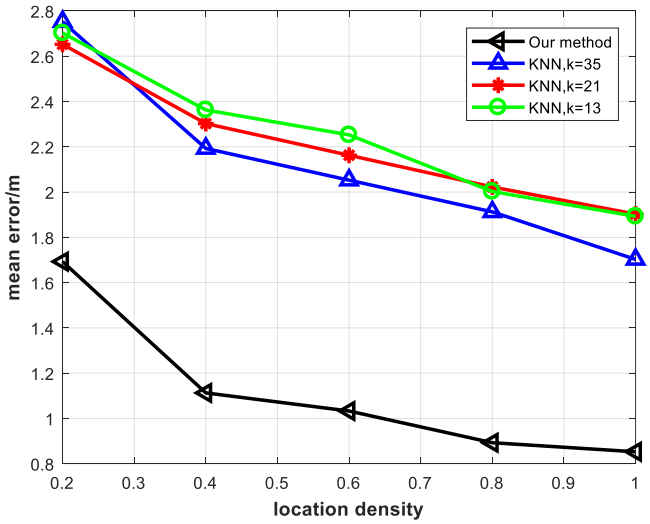

(b) The second floor

Figure 5.5 Average error at different position densities

Figure 5.5 shows the average positioning position errors of this method and the comparison algorithm under different position densities. The position density is expressed as the ratio of the size of the area occupied by the selected data to the total area size. As can be seen under the same position density, the average error of the proposed method has higher accuracy than that of the comparison algorithm using the same data set. In addition, when the position density reaches 1, that is, all data are selected, and the average position error of the algorithm in this research is 0.86m. Compared with the

IJARCCE ISSN (O) 2278-1021, ISSN (P) 2319-5940

International Journal of Advanced Research in Computer and Communication Engineering

Impact Factor 8.102 ⁜ Peer-reviewed & Refereed journal ⁜ Vol. 13, Issue 11, November 2024

DOI: 10.17148/IJARCCE.2024.131101

same position density, the best average error of the comparison algorithm is 1.72m.

Table 5.1 Comparison of error of different methods

Methods	Avarage distance error
Our method	0.86m
KNN, k=35	1.72m
KNN, k=21	1.84m
KNN, k=13	1.86m

T. CONVERGENCE ANALYSIS

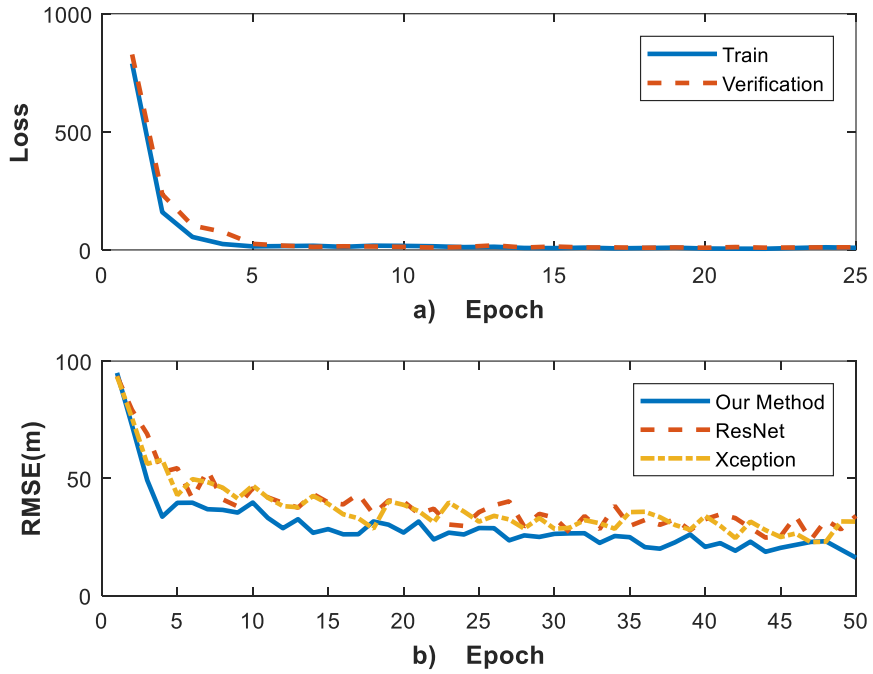

Figure 5.6 (a) Loss on the training and test sets (b) Convergence comparison for the first 50 training cycles

Convergence testing is required to evaluate the performance and structure of DNNS. The loss of the algorithm proposed in this research on the training set and the test set is shown in Figure 5.6 (a). In the first 25 training cycles, the algorithm loss proposed in this research decreases from 763.37 to 5.31. At the same time, the curve on the test set is always close to the curve on the training set during the whole training process, indicating that no overfitting has occurred. In addition, two classical DNN algorithms, ResNet-18**Error! Reference source not found.** and Xception**Error! Reference source not found.**, are compared to calculate the convergence rate of position mean error. As shown in Figure 5.6 (b), the convergence rate of the proposed algorithm is better than ResNet and Xception, because parallel path processing and PCA algorithm can greatly reduce the computational workload. At the same time, the algorithm proposed in this research has fewer peaks and fluctuations, so it also has advantages in terms of fast convergence and stability.

IJARCCE ISSN (O) 2278-1021, ISSN (P) 2319-5940

International Journal of Advanced Research in Computer and Communication Engineering

Impact Factor 8.102 ⁜ Peer-reviewed & Refereed journal ⁜ Vol. 13, Issue 11, November 2024

DOI: 10.17148/IJARCCE.2024.131101

U. TIME COMPLEXITY

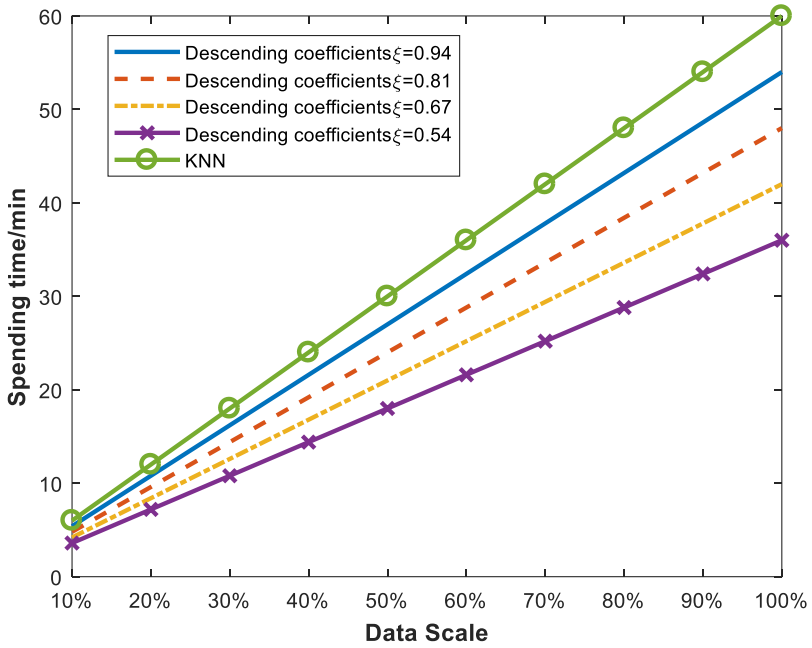

Figure 5.7 Training time overhead with different dataset sizes

Figure 5.7 shows the training time cost of the proposed method on data sets of different scales. The iteration number set by the algorithm is 500, and it is found that the change of time consumption is basically linear. When using the WKNN method, 1000 training clusters. The training time was 60 minutes. The proposed algorithm can reduce the training time by adjusting the reduced maintenance number of PCA. As shown in Figure 5.7, when the drop maintenance number decreases from 0.94 to 0.54, the training time of 1000 training sets decreases from 54 minutes to 36 minutes. In addition, this work tested the time spent on position estimation. After training, DNN model parameters, it took less than 14 minutes to invert the positions of 470 measuring points on the third floor of the data set, that is, the position inversion of each measuring point was less than 1.8 seconds. This proves that the method proposed in this research can be used to rapidly estimate the measurement position of mobile terminals.

V. SIMILARITY ANALYSIS

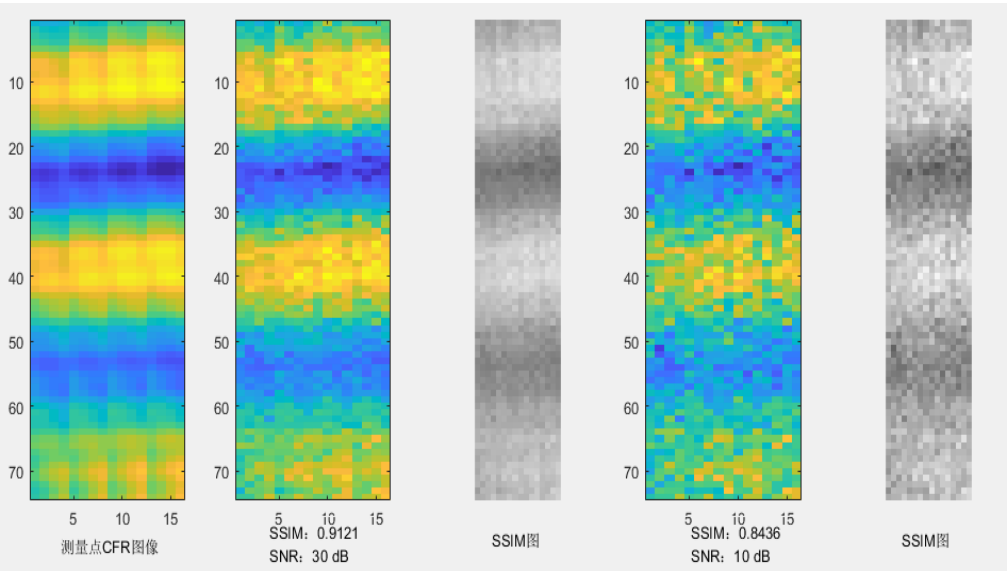

Figure 5.8 the leftmost CFR image is the real CFR image, and the latter two are the composite CFR image and SSIM image.

IJARCCE ISSN (O) 2278-1021, ISSN (P) 2319-5940

International Journal of Advanced Research in Computer and Communication Engineering

Impact Factor 8.102 ⁜ Peer-reviewed & Refereed journal ⁜ Vol. 13, Issue 11, November 2024

DOI: 10.17148/IJARCCE.2024.131101

Since the method proposed in this research is to synthesize the FTTR scene data set by using the existing WiFi fingerprint data set, it is necessary to verify the difference between the synthesized data set and the real data set, and such difference is estimated by the structural similarity of the data set. In order to compare the synthesized frequency response image with the corresponding sampled frequency response image, as shown in Figure 5.9, measuring point No. 10 is randomly selected from the test point on the third floor of the data set to measure the frequency response image generated by WiFi access point No.3. As shown in Figure 5.8, the leftmost is the frequency response image actually measured, and the other two are the frequency response image synthesized by the test point under SNR=30dB and 10dB, respectively. It can be found that the brightness and local similarity of each pixel in the synthesized image are similar to the image actually measured. In order to quantitatively compare the consistency between the synthesized image and the measured image, it can be calculated that the average SSIM is 0.9121 when SNR=30dB and 0.8436 when SNR=10dB. Theoretically, the average SSIM of the measured image is 1, which indicates that under the condition of high signal-noise ratio. The synthetic frequency response image method adopted in this paper can effectively fit the measured results.

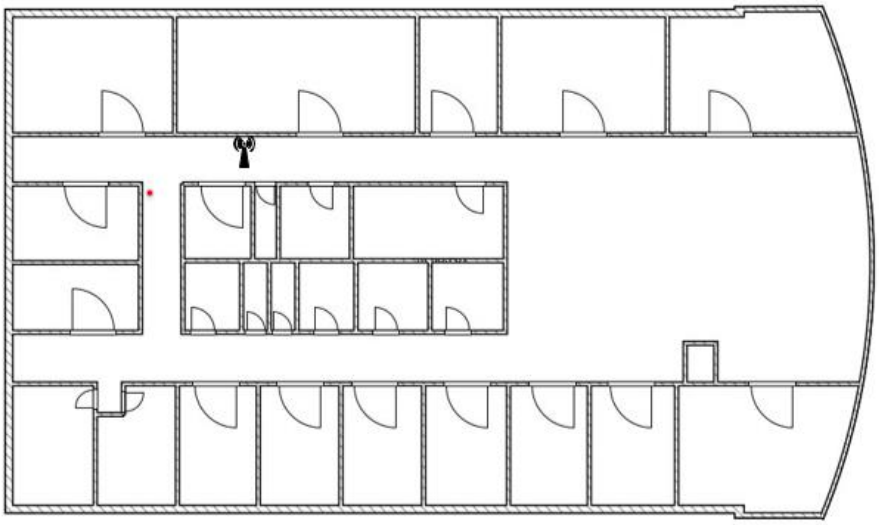

Figure 5.9 Location map of measurement point 10 and WiFi access point No. 3

CONCLUTION AND FUTURE WORK

W. SUMMARY

In summary, the creation of a WiFi-based high-precision indoor positioning scheme for FTTR scenarios has significant promise for improving location accuracy and opening up a variety of applications. This plan takes advantage of the current WiFi network, making it a reasonably priced method of interior placement. It outperforms conventional WiFi-based systems in terms of positioning accuracy through a mix of signal strength fingerprinting and machine learning methods. The method deals with the difficulties of interior positioning in FTTR settings, where the presence of barriers and multipath effects can dramatically impair positioning performance. It efficiently reduces the impact of these factors, leading to increased accuracy, by implementing a thorough fingerprinting database and utilizing cutting-edge machine learning techniques.

The location estimate of multiple indoor Wi-Fi access points in FTTR situations is addressed in this research, and we also provide a method for assembling the frequency response image of FTTR scenarios using the 2.4GHz Wi-Fi fingerprint datasets that are already available. Using frequency response images as a starting point, a deep learning localization system was created using PCA analysis of parallel routes in the training stage and DNN inversion in the placement step. According to the simulation results, the position inversion algorithm based on frequency response images has a training time that is much shorter than the traditional DNN algorithm and a positioning accuracy that is around 15 to 29% higher than that of the conventional algorithm. Thus, when compared to other cutting-edge approaches, the algorithm suggested in this study offers clear advantages. The study on adaptability to environmental noise needs to be processed promptly because this work uses the current Wi-Fi fingerprint data set to synthesize the FTTR scene data set and does not characterize the distance characteristics of FTTR access points and mobile terminal devices. The proposed method and the designed positioning algorithm's accuracy will both be improved in further work.

DOI: 10.17148/IJARCCE.2024.131101

X. PROSPECT for FUTURE RESEARCH

For the past few years, indoor positioning, or indoor localization, has been the focus of intense study and development. Future research in this area has a number of avenues that could be pursued, some of which are described below and many more.

- Privacy and security: As indoor positioning systems proliferate, issues about privacy and security will surface. The development of safe and private indoor positioning systems that safeguard user data will be the main goal of future research in this area.

- Integration with robots: Indoor positioning systems can be utilized to make indoor environments suitable for robots. Robots can be fitted with sensors that provide positional data, enabling them to roam independently and complete jobs more quickly.

There are, nevertheless, a number of regions in need of further development. First, more research may be done to improve the fingerprinting procedure and strengthen the scheme's resistance to environmental changes and dynamic network conditions. This can entail looking into more sophisticated machine learning techniques or adding extra sensor data, like that from Bluetooth beacons or inertial sensors, to improve positioning precision.

In conclusion, there are a lot of potential future works for indoor positioning or indoor localization, researchers and developers in this sector are continually looking into new concepts and technologies to enhance the precision, effectiveness, and utility of these systems.

REFERENCES

[1] ITU-T, "GSTP-FTTR Use cases and requirements of fibre-to-theroom (FTTR)," ITU-T Technical Paper, April 2021.
[2] Nishimoto K, Tochino T, Hatano T, et al. Mini-PON: disaggregated module-type PON architecture for realizing various PON deployments[J]. Journal of Optical Communications and Networking, 2020, 12(5): 89-98.
[3] Pfeiffer T, Dom P, Bidkar S, et al. PON going beyond FTTH [Invited Tutorial][J]. Journal of Optical Communications and Networking, 2022, 14(1): A31-A40.
[4] Yeh C H, Wang B Y, Hsu W H, et al. A simple WDM-PON architecture together with private interconnected ONUs[J]. IEEE Access, 2021, 9: 126319-126323.
[5] 张晓兰. GPON 技术及其在宽带接入网中的技术应用[D]. 战略支援部队信息工程大学, 2019.
[6] Dutta S, Roy D, Das G. Protocol Design for Energy Efficient OLT in TWDM-EPON Supporting Diverse Delay Bounds[J]. IEEE Transactions on Green Communications and Networking, 2021, 5(3): 1438-1450.
[7] Dutta S, Roy D, Das G. SLA-aware protocol design for energy-efficient OLT transmitter in TWDM-EPON[J]. IEEE Transactions on Green Communications and Networking, 2021, 5(4): 1961-1973.
[8] Echraibi A, Flocon-Cholet J, Gosselin S, et al. Deep Infinite Mixture Models for Fault Discovery in GPON-FTTH Networks[J]. IEEE Access, 2021, 9: 90488-90499.
[9] Uzawa H, Honda K, Nakamura H, et al. Dynamic bandwidth allocation scheme for network-slicing-based TDM-PON toward the beyond-5G era[J]. Journal of Optical Communications and Networking, 2020, 12(2): A135-A143.
[10] Lee H H, Kim K O, Doo K H, et al. Demonstration of high-power budget TDM-PON system with 50 Gb/s PAM4 and saturated SOA[J]. Journal of Lightwave Technology, 2021, 39(9): 2762-2768.
[11] Li B, Zhang K, Zhang D, et al. DSP enabled next generation 50G TDM-PON[J]. Journal of Optical Communications and Networking, 2020, 12(9): D1-D8.
[12] He Y, Chen Y, Hu Y, et al. WiFi vision: Sensing, recognition, and detection with commodity MIMO-OFDM WiFi[J]. IEEE Internet of Things Journal, 2020, 7(9): 8296-8317.
[13] Li Y, Barthelemy J, Sun S, et al. A case study of WiFi sniffing performance evaluation[J]. IEEE Access, 2020, 8: 129224-129235.
[14] Tan S, Ren Y, Yang J, et al. Commodity WiFi Sensing in Ten Years: Status, Challenges, and Opportunities[J]. IEEE Internet of Things Journal, 2022, 9(18): 17832-17843.
[15] Chen L, Wang Z, Du Y, et al. Generalized transceiver beamforming for DFRC with MIMO radar and MU-MIMO communication[J]. IEEE Journal on Selected Areas in Communications, 2022, 40(6): 1795-1808.
[16] Liu X, Huang T, Shlezinger N, et al. Joint transmit beamforming for multiuser MIMO communications and MIMO radar[J]. IEEE Transactions on Signal Processing, 2020, 68: 3929-3944.
[17] Xie D, Zhang J, Tang A, et al. Multi-dimensional busy-tone arbitration for OFDMA random access in IEEE 802.11 ax[J]. IEEE Transactions on Wireless Communications, 2020, 19(6): 4080-4094.

DOI: 10.17148/IJARCCE.2024.131101

[18] Cheng R G, Yang C M, Firmansyah B S, et al. Uplink OFDMA-Based Random Access Mechanism With Bursty Arrivals for IEEE 802.11 ax Systems[J]. IEEE Networking Letters, 2021, 4(1): 34-38.
[19] Bahl P, Padmanabhan V N. RADAR: An in-building RF-based user location and tracking system[C]//Proceedings IEEE INFOCOM 2000. Conference on computer communications. Nineteenth annual joint conference of the IEEE computer and communications societies (Cat. No. 00CH37064). Ieee, 2000, 2: 775-784.
[20] Oh J, Kim J. AdaptiveK-nearest neighbour algorithm for WiFi fingerprint positioning[J]. Ict Express, 2018, 4(2): 91-94.
[21] Y. Xie, Y. Wang, A. Nallanathan, and L. Wang, "An improved K-nearest-neighbor indoor localization method based on spearman distance," IEEE Signal Process. Lett., vol. 23, no. 3, pp. 351–355, Mar. 2016.
[22] Wu Z, Fu K, Jedari E, et al. A fast and resource efficient method for indoor positioning using received signal strength[J]. IEEE Transactions on Vehicular Technology, 2016, 65(12): 9747-9758.
[23] Figuera C, Rojo-Álvarez J L, Wilby M, et al. Advanced support vector machines for 802.11 indoor location[J]. Signal Processing, 2012, 92(9): 2126-2136.
[24] Khatab Z E, Hajihoseini A, Ghorashi S A. A fingerprint method for indoor localization using autoencoder based deep extreme learning machine[J]. IEEE sensors letters, 2017, 2(1): 1-4.
[25] Zou H, Huang B, Lu X, et al. A robust indoor positioning system based on the procrustes analysis and weighted extreme learning machine[J]. IEEE Transactions on Wireless Communications, 2015, 15(2): 1252-1266.
[26] Zou H, Lu X, Jiang H, et al. A fast and precise indoor localization algorithm based on an online sequential extreme learning machine[J]. Sensors, 2015, 15(1): 1804-1824.
[27] Wu K, Xiao J, Yi Y, et al. CSI-based indoor localization[J]. IEEE Transactions on Parallel and Distributed Systems, 2012, 24(7): 1300-1309.
[28] Yang Z, Zhou Z, Liu Y. From RSSI to CSI: Indoor localization via channel response[J]. ACM Computing Surveys (CSUR), 2013, 46(2): 1-32.
[29] Wang X, Gao L, Mao S. CSI phase fingerprinting for indoor localization with a deep learning approach[J]. IEEE Internet of Things Journal, 2016, 3(6): 1113-1123.
[30] Wang X, Gao L, Mao S, et al. DeepFi: Deep learning for indoor fingerprinting using channel state information[C]//2015 IEEE wireless communications and networking conference (WCNC). IEEE, 2015: 1666-1671.
[31] Song Q, Guo S, Liu X, et al. CSI amplitude fingerprinting-based NB-IoT indoor localization[J]. IEEE Internet of Things Journal, 2017, 5(3): 1494-1504.
[32] Wang Y, Xiu C, Zhang X, et al. WiFi indoor localization with CSI fingerprinting-based random forest[J]. Sensors, 2018, 18(9): 2869.
[33] Shi S, Sigg S, Chen L, et al. Accurate location tracking from CSI-based passive device-free probabilistic fingerprinting[J]. IEEE Transactions on Vehicular Technology, 2018, 67(6): 5217-5230.
[34] Luo R C, Hsiao T J. Dynamic wireless indoor localization incorporating with an autonomous mobile robot based on an adaptive signal model fingerprinting approach[J]. IEEE Transactions on Industrial Electronics, 2018, 66(3): 1940-1951.
[35] Chen C, Chen Y, Han Y, et al. Achieving centimeter-accuracy indoor localization on WiFi platforms: A multi-antenna approach[J]. IEEE Internet of Things Journal, 2016, 4(1): 122-134.
[36] Magsino E R, Ho I W H, Situ Z. The effects of dynamic environment on channel frequency response-based indoor positioning[C]//2017 IEEE 28th Annual International Symposium on Personal, Indoor, and Mobile Radio Communications (PIMRC). IEEE, 2017: 1-6.
[37] Tseng P H, Chan Y C, Lin Y J, et al. Ray-tracing-assisted fingerprinting based on channel impulse response measurement for indoor positioning[J]. IEEE Transactions on Instrumentation and Measurement, 2017, 66(5): 1032-1045.
[38] Jeon N R, Lee C, Kang N G, et al. Performance of channel prediction using 3D ray-tracing scheme compared to conventional 2D scheme[C]//2006 Asia-Pacific Conference on Communications. IEEE, 2006: 1-6.
[39] Nagaraj S, Khan S, Schlegel C, et al. Differential preamble detection in packet-based wireless networks[J]. IEEE Transactions on Wireless Communications, 2009, 8(2): 599-607.
[40] Yan J, Qi G, Kang B, et al. Extreme Learning Machine for Accurate Indoor Localization Using RSSI Fingerprints in Multifloor Environments[J]. IEEE Internet of Things Journal, 2021, 8(19): 14623-14637.
[41] Rambhatla S, Li X, Ren J, et al. A dictionary-based generalization of robust PCA with applications to target localization in hyperspectral imaging[J]. IEEE Transactions on Signal Processing, 2020, 68: 1760-1775.
[42] Njima W, Bazzi A, Chafii M. DNN-based indoor localization under limited dataset using GANs and semi-supervised learning[J]. IEEE Access, 2022, 10: 69896-69909.
[43] Chen C Y, Alexander I, Lai C, et al. Optimization and Evaluation of Multidetector Deep Neural Network for High-Accuracy Wi-Fi Fingerprint Positioning[J]. IEEE Internet of Things Journal, 2022, 9(16): 15204-15214.
[44] Shi J, Wang G, Jin L. Least squared relative error estimator for RSS based localization with unknown transmit power[J]. IEEE Signal Processing Letters, 2020, 27: 1165-1169.

International Journal of Advanced Research in Computer and Communication Engineering
Impact Factor 8.102 ⁜ Peer-reviewed & Refereed journal ⁜ Vol. 13, Issue 11, November 2024
DOI: 10.17148/IJARCCE.2024.131101

[45] Watanabe F. Wireless sensor network localization using AoA measurements with two-step error variance-weighted least squares[J]. IEEE Access, 2021, 9: 10820-10828.
[46] Tóth Z, Tamás J. Miskolc IIS hybrid IPS: Dataset for hybrid indoor positioning[C]//2016 26th International Conference Radioelektronika (RADIOELEKTRONIKA). IEEE, 2016: 408-412.
[47] Wei W, Yan J, Wu X, et al. CSI fingerprinting for device-free localization: Phase calibration and SSIM-based augmentation[J]. IEEE Wireless Communications Letters, 2022, 11(6): 1137-1141.
[48] Li S, Lei W, Zhang W, et al. Weighted TSVR based nonlinear channel frequency response estimation for MIMO-OFDM system[J]. IEEE Access, 2020, 8: 224283-224291.
[49] Thenuardi D, Soewito B. Indoor Positioning System using WKNN and LSTM Combined via Ensemble Learning[J]. Advances in Science, Technology and Engineering Systems Journal, 2020, 6: 242-249.
[50] He K, Zhang X, Ren S, et al. Deep residual learning for image recognition[C]//Proceedings of the IEEE conference on computer vision and pattern recognition. 2016: 770-778.
[51] Chollet F. Xception: Deep learning with depthwise separable convolutions[C]//Proceedings of the IEEE conference on computer vision and pattern recognition. 2017: 1251-1258.

